NASA TECHNICAL NOTE

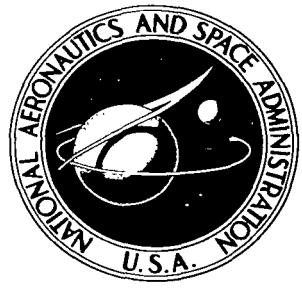

NASA TN D-2048

C. 1

NASA TN D-2048

BOUNDARY-LAYER VELOCITY PROFILES AND SKIN FRICTION DUE TO SURFACE ROUGHNESS ON AN OGIVE CYLINDER AT MACH NUMBERS OF 1.61 AND 2.01

by K. R. Czarnecki and William J. Monta

Langley Research Center
Langley Station, Hampton, Va.

NATIONAL AERONAUTICS AND SPACE ADMINISTRATION • WASHINGTON, D. C. • DECEMBER 1963

TECHNICAL NOTE D-2048

BOUNDARY-LAYER VELOCITY PROFILES AND SKIN FRICTION DUE TO SURFACE ROUGHNESS ON AN OGIVE CYLINDER AT MACH NUMBERS OF 1.61 AND 2.01

By K. R. Czarnecki and William J. Monta

Langley Research Center
Langley Station, Hampton, Va.

NATIONAL AERONAUTICS AND SPACE ADMINISTRATION

BOUNDARY-LAYER VELOCITY PROFILES AND SKIN FRICTION DUE TO SURFACE ROUGHNESS ON AN OGIVE CYLINDER AT MACH NUMBERS OF 1.61 AND 2.01

By K. R. Czarnecki and William J. Monta

SUMMARY

An investigation has been made at Mach numbers of 1.61 and 2.01 and over a range of free-stream Reynolds number per foot from about 2.4×10^6 to 7.1×10^6 to determine the boundary-layer velocity profiles and skin-friction drags due to two-dimensional fabrication-type surface roughness. Nine types of surface roughness, including step, wave, crease, and swept configurations were investigated. The tests were made on an ogive cylinder of fineness ratio 12.2, the roughness elements covering the cylindrical portion of the model.

The results indicate that the velocity profiles for both the smooth models and models with surface roughness (exclusive of those for the models with the largest roughness, and for which the data cannot be interpreted) tend toward agreement with the 1/7- and 1/8-power velocity distributions. Surface roughness up to a height of 0.021 inch, at least, had only a small effect on the boundary-layer momentum losses. The tests confirm the conclusion previously established that surface roughness apparently has only a small effect on skin friction and that wave drag probably constitutes at least the major part of the drag of surface roughness, as determined by balance tests.

INTRODUCTION

As the designs of supersonic aircraft become more refined, the proportion of the airplane drag assignable to skin friction generally increases. This fact makes it imperative, from the standpoint of obtaining optimum performance in speed and range, that the airplane skin friction be maintained at the lowest practical value by keeping the airplane surfaces aerodynamically smooth. In actual practice the aerodynamically smooth surface is difficult to achieve, and a certain amount of surface roughness in the form of waviness, steps, grooves, and similar protuberances must be accepted. In order to determine the relative magnitude of the skin friction due to roughness that may be encountered at supersonic speeds and to learn something about the basic flow mechanisms involved, a general investigation of fabrication-type roughness is being made over a wide range of Mach numbers and Reynolds numbers at the Langley Research Center. Because most of the boundary-layer flow on an airplane will be turbulent, the investigation is primarily concerned with the turbulent boundary layer. The investigation includes force tests,

surface pressure distributions, and boundary-layer profile surveys. Some of the force-test results have been presented in reference 1; results from the surface-pressure investigation have been reported in reference 2. This paper presents the results from the boundary-layer profile surveys.

The profile surveys were made on nine types of fabrication roughness built into the cylindrical portion of an ogive cylinder with a fineness ratio of 12.2 and on a smooth-surface reference model. The tests were made at nominal Mach numbers of 1.61 and 2.01 and over a range of free-stream Reynolds number per foot from about 2.4×10^6 to 7.1×10^6. The model axis was always alined with the stream with transition artificially fixed near the model nose.

SYMBOLS

C_F average skin-friction coefficient, $\frac{\text{Friction drag}}{q_\infty S_W} = 2\Theta_{corr} \frac{2\pi r}{S_W}$

M Mach number

q dynamic pressure

R_{ft} free-stream Reynolds number per foot

R_x Reynolds number based on axial distance from model nose

r model radius measured normal to body axis

R radius of model ogive

S_W wetted surface area

u velocity

x axial distance from model nose

y distance normal to model surface

δ boundary-layer thickness

Θ three-dimensional momentum thickness, $\int_0^\delta \frac{\rho u}{\rho_\delta u_\delta}\left(1 - \frac{u}{u_\delta}\right)\left(1 + \frac{y}{r}\right)dy$

ρ density

Subscripts:

δ	local conditions just outside the boundary layer
∞	free stream
corr	corrected to 48-inch axial station

APPARATUS AND METHODS

Wind Tunnel

This investigation was conducted in the Langley 4- by 4-foot supersonic pressure tunnel. From calibrations made specifically for these tests, it was found that the mean test-section Mach number in the region of the model location decreased as the tunnel stagnation pressure was decreased. For the worst case, nominal Mach number of 2.01, the Mach number decreased by almost 0.01 at a stagnation pressure of 10 pounds per square inch absolute from the value measured at a stagnation pressure of 30 pounds per square inch absolute.

Models and Instrumentation

A 50.0-inch-long 4.096-inch-diameter 3-caliber-nose ogive cylinder was the basic configuration of the 10 sting-mounted models used in this investigation. (See fig. 1.) The reference model had a smooth surface with no roughness elements. The remaining nine configurations were smooth on the ogive sections, but each had a number of cycles of a particular type of fabrication roughness constructed into the cylindrical portion of the body. (See figs. 2 and 3.) These roughness cycles included forward-facing steps, rearward-facing steps, steps with grooves, creases, and protruding waves - each having a nearly constant cycle length of 1.5 to 4.0 inches, and a constant height of 0.014 to 0.053 inch. The heights of the various roughness elements were selected to be representative of fabrication imperfections found on recent production transonic aircraft of aluminum construction, and the cycle lengths were chosen to provide enough cycles on the models (table I) so that a measurable difference in drag would be obtainable in balance tests (the results for some of which were previously reported in ref. 1). On seven of these models the roughness cycles were wrapped around the model unswept; on the remaining two, they were swept 45°. The relationship of the maximum roughness height to the estimated total boundary-layer thickness is shown in figure 4 for $M_\infty = 1.61$. There was only a slight change for $M_\infty = 2.01$. The test models were made of wood covered with Paraplex and fiber glass. The first 2 inches of the nose of each of the fabrication-roughness ogive cylinders was aluminum in order to minimize tip damage. The surface finish of all models was very smooth, usually less than 10 microinches. Small-scale waviness was often present on the models, superimposed on some of the roughness cycles. Although this condition prevented all cycles on any model from being identical, the deviations from the desired contours were generally so few and small that they are believed to have no influence upon the conclusions drawn from these tests.

Each model, except for the one used to determine the smooth-surface reference profiles, was instrumented with a number of static-pressure orifices in a single row parallel to the model center line. On the fabrication-roughness ogive cylinders the orifices were usually located along the second and next-to-last cycles of roughness in the approximate areas indicated in figure 1. Inasmuch as no pressures measured by these orifices are shown directly in this report, the details of the orifice installations are omitted, but can be found in reference 2. Details of the orifice installations used to determine the pressure distributions for the smooth-surface reference condition can also be found in this reference.

The total pressure within the boundary layer was determined by means of a pitot tube attached to a driving mechanism that in turn was mounted on an auxiliary sting. Both forward and rearward motion, as well as motion normal to the model surface, could be provided in very small increments (0.001 inch or less). The pitot tube had a normal outside diameter of 0.070 inch and a wall thickness of 0.005 inch but the front end was flattened to a slit about 0.002 or 0.003 inch wide, and the walls were honed to a thickness of approximately 0.002 inch. The pitot tube was connected to a pressure transducer the output of which was led into a servomechanism through which the reading was punched on an IBM card. No static pressures were measured within the boundary layer.

Other instrumentation consisted of an Alkazene (specific gravity of 1.75) manometer board to register model pressures, a 9-inch camera to photograph the manometer board, and several Ideal manometers for measuring reference pressures.

Test Conditions

All tests were made at an angle of incidence of 0° with a fully turbulent boundary layer, transition being promoted by sand grain roughness (usually number 24 or 46) cemented to the model 1 inch from the tip. All data were obtained with the tunnel conditions held in equilibrium. During all runs the dewpoint temperature was maintained low enough to prevent condensation effects.

Range of Tests

Tests were made on each model at nominal Mach numbers of 1.61 and 2.01. Boundary-layer profiles were determined only on roughness cycles not too far from the model base - in the area of from about 45.3 to 48.6 inches from the model nose. When possible, the profiles were determined on that part of the roughness cycle where the surface static-pressure distributions of reference 2 indicated an approximately zero pressure gradient. (See table I for profile station locations.) On a few configurations a small number of additional profiles were determined in alternate areas. Data usually were taken at increments of 5 pounds per square inch in stagnation pressure between 10 and 25 pounds per square inch absolute. These values correspond to a range of Reynolds number per foot of 2.8×10^6 to 7.0×10^6 at $M = 1.61$ and 2.4×10^6 to 6.0×10^6 at $M = 2.01$. On the smooth reference ogive cylinder an additional profile was obtained at $M = 2.01$ at $R_{ft} = 7.08 \times 10^6$. Stagnation temperatures were $110^\circ \pm 2^\circ$ F.

Data Reduction

Boundary-layer total pressures were reduced to velocity profiles by assuming that the static pressures through the boundary layer were constant and equal to those measured on the model surface at the profile measuring stations. A constant stagnation temperature equal to the free-stream value was also assumed. Reduction to velocity ratios was accomplished by the use of the local velocity just outside the boundary layer at the measuring station as the reference.

Momentum thicknesses were computed by accounting for the cylindrical form of the models at the measuring stations by the method of reference 3. Local conditions just outside the boundary layer were used as the reference values. The use of local conditions automatically excludes any wave drag originating at the model nose, except for rotational-flow effects stemming from changes in shock curvature along the shock front, from being included in the boundary-layer momentum losses. Theoretical considerations and the constant velocity ratios found outside the boundary layer in the case of the smooth model as the distance from the surface increases (figs. 5(a) and 6(a)) indicate that this rotational-flow effect is negligible. For the models with surface roughness, the wave drag from the roughness elements should cause some change in local Mach numbers with reference to the smooth reference model. No such changes could be discerned because all the local Mach numbers were practically identical to one another, exclusive of those for the models with the 0.053-inch roughness, which are considered unreliable. Apparently this loss in momentum is distributed over such a large area at the measuring station that the changes in local conditions are within experimental accuracy. Thus, the momentum loss due to roughness wave drag that is included in the boundary-layer momentum surveys is very small. Use of local conditions as reference for the determination of Θ results in the momentum thickness being referenced to the local conditions, but in these tests the local Mach numbers (exclusive of those for the 0.053-inch roughness models) were so close to the free-stream value that no changes had to be made to Θ to convert it to free-stream condition.

In order to compare skin-friction values for the various roughness configurations on the basis of a common or reference length, it was assumed that the growth of the momentum thickness Θ with model length could be expressed by

$$\Theta = K\left(R_x\right)^{4/5} \tag{1}$$

where K is a constant for any one model. The momentum thicknesses were then corrected to the common reference station of 48 inches, the station where the profile was measured on the smooth model, by the following formula derived from equation (1) for constant R_{ft}.

$$\Theta_{corr} = \Theta\left(\frac{48}{x}\right)^{4/5} \tag{2}$$

where x represents the length to the profile measuring station in inches. The average skin-friction coefficients were found from

$$C_F = \frac{\text{Friction drag}}{q_\infty S_W} \tag{3}$$

Drag is equal to the time rate change of momentum completely around the body at the measuring station. In equation form

$$C_F = \frac{2\pi \int_0^{\delta} \rho u \left(u_\delta - u\right)\left(r + y\right) dy}{q_\infty S_W} \tag{4}$$

With the normalization of ρ and u by the reference quantities ρ_δ and u_δ, and the use of the definition for Θ, equation (4) is converted to

$$\left.\begin{aligned} C_F &= 2\Theta\left(\frac{2\pi r}{S_W}\right)\left(\frac{q_\delta}{q_\infty}\right) \\ \text{or} \qquad C_F &= 2\Theta\,\frac{2\pi r}{S_W} \end{aligned}\right\} \tag{5}$$

inasmuch as q_δ was equal to q_∞ within experimental error. In order to make the comparison at a common station, Θ_{corr} was used in equation (5) to yield

$$C_F = 2\Theta_{corr}\,\frac{2\pi r}{S_W} \tag{6}$$

RESULTS AND DISCUSSION

Boundary-Layer Velocity Profiles

Some typical boundary-layer velocity profiles, plotted in the nondimensional form of u/u_δ as a function of y/Θ, are presented in figures 5 and 6 for the test Mach numbers of 1.61 and 2.01, respectively. Figures 5(a) and 6(a) present boundary-layer profiles determined on the smooth reference models. Figures 5(b), 5(c), 5(d), and 6(b), 6(c), and 6(d) illustrate the type of boundary-layer profiles found on most surface-roughness configurations. Finally, figures 5(e), 5(f), and 6(e), 6(f) show the boundary-layer profiles determined on the two models with the greatest height of surface roughness - the models with the 0.053 transverse creases and 0.053 protruding waves.

With the exception of those for the models with 0.053-inch roughness, the boundary-layer velocity profiles for the various roughness configurations closely resemble one another and the profiles for the smooth reference model. In the case of the 0.053-inch roughness configurations, there was obviously a variation in static pressure through the boundary layer, and it was not possible to determine accurately the true edge of the boundary layer or the correct external local velocity. As illustrated in figure 6(f), attempts to determine the profiles at another axial station did not resolve this difficulty. A comparison of the boundary-layer profiles for the smooth models at the highest and lowest test

values of R_{ft} with calculated 1/7- and 1/8-power profiles is presented in figures 7 and 8. The comparison indicates that at the lowest test R_{ft} values the experimental boundary-layer profiles tend to be in agreement with the 1/7-power velocity distributions. At the highest test values of R_{ft} the experimental profiles tend toward agreement with the 1/8-power profiles. Inasmuch as the profiles for the various roughness configurations (exclusive of those for the 0.053-inch surface roughness) are similar to those of the smooth reference models, they also tend toward agreement with the 1/7- and 1/8-power velocity distributions. Because of this agreement of the experimental velocity profiles with the calculated 1/7- and 1/8-power profiles, which past tests have established for this test Reynolds number range for smooth surfaces (for example, see ref. 3), it is believed that these boundary-layer velocity profiles are sufficiently reliable to determine boundary-layer momentum losses with reasonable accuracy. This statement, of course, does not apply to the 0.053-inch surface-roughness configurations.

Boundary-Layer Momentum Thicknesses

The boundary-layer momentum thicknesses determined from the profile surveys are presented in figures 9 and 10. In figures 11 and 12 are presented the momentum thicknesses corrected to the smooth-model measurement station of 48 inches. In all figures a comparison is made of the experimental results with theoretical curves derived from the T' method of reference 4 for a 48-inch flat plate. It was felt that both experimental accuracy and the lack of a suitable method did not warrant correcting the theoretical flat-plate momentum thicknesses for the ogive-cylinder shape of the test models.

A comparison of figure 9 with figure 11, and figure 10 with figure 12, indicates that the correction of the experimental values of Θ to a common reference station has a negligible effect on the overall trends. In general, the bulk of the experimental results tends to be somewhat below the theoretical curves. For the smoother configurations this result is to be expected because of the thinning effect of both the ogive nose section and the cylindrical flow. At $M_\infty = 1.61$, the experimental results for the smooth model lie near the bottom of the band of data that are considered reliable, as might be expected. At $M_\infty = 2.01$, the experimental data for this configuration tend toward the center of the band, and thus indicate only a small decrease in skin friction with Mach number for this reference smooth-body case. In view of some of the random variations between models at the two test Mach numbers and the fact that the bulk of the data do indicate the proper Mach number trend, it is believed that this discrepancy in the smooth-body data is the result of experimental inaccuracies. Inspection of the probe after the $M_\infty = 2.01$ smooth-body tests indicated that the probe had been damaged. It is possible that the experimental momentum thicknesses for all test configurations may be within experimental accuracy, but there appears to be a general tendency for somewhat greater momentum thicknesses for models with the larger and unswept surface roughnesses. Data for the 0.053-inch roughness models are obviously unreliable, as illustrated by the abnormally low values of Θ determined for the model with 0.053 protruding waves at $M = 1.61$ and the large changes Θ found for the same model at $M = 2.01$ for a slightly different profile measurement station (flagged vs. unflagged symbols). The conclusion can be made, therefore, that fabrication-type surface roughness up to a height of 0.021 inch at least, will have only small effect on the boundary-layer momentum losses.

Skin-Friction Coefficients

In order to simplify the comparison of the present results with previous force tests, the boundary-layer momentum thicknesses have been converted to average skin-friction coefficients based on free-stream conditions and wetted surface area for the station length of 48 inches in figures 13 and 14. Comparison with theory (flat-plate T' method for the 48-inch station) is also provided for the smooth-surface reference models. Included in figures 13 and 14 are curves representing skin-friction data obtained on the smooth-surface model by means of force tests (ref. 1 and unpublished data). No attempt was made to correct the momentum skin-friction coefficients to the full 50-inch length of the force-test models.

A comparison of the experimental results of figures 13 and 14 for the various roughness configurations with the force-test results of reference 1 and with unpublished data indicates that surface roughness apparently has only a small effect on skin friction and that roughness wave drag probably constitutes at least the major part of the drag of surface roughness elements as determined by balance tests. This conclusion corroborates the one made in reference 2 from a comparison of measured wave drags with corresponding force tests. The skin-friction coefficients derived from the momentum surveys for the smooth configuration are approximately 10 percent below the force-test data. The discrepancy is probably the result of using only one boundary-layer survey station for each model. The force tests, which are probably more reliable, indicate that the drag of an ogive cylinder may be approximately 10 percent higher than that indicated by flat-plate theory in this test Mach number and Reynolds number range because of three-dimensional boundary-layer flow effects.

CONCLUSIONS

An investigation has been made to determine the boundary-layer velocity profiles and skin friction due to two-dimensional fabrication-type surface roughness on an ogive cylinder at Mach numbers of 1.61 and 2.01 and over a free-stream Reynolds number per foot range from about 2.4×10^6 to 7.1×10^6. The results indicate that the velocity profiles for both the smooth models and models with surface roughness (exclusive of those for the models with the largest roughness and for which the data cannot be interpreted) tend toward agreement with the 1/7- and 1/8-power velocity distributions. Surface roughness up to a height of 0.021 inch at least had only a small effect on the boundary-layer momentum losses. The tests confirm the conclusion previously established that surface roughness apparently has only a small effect on skin friction and that roughness wave drag probably constitutes at least the major part of the drag of surface-roughness elements as determined by balance tests.

Langley Research Center,
National Aeronautics and Space Administration,
Langley Station, Hampton, Va., September 6, 1963.

REFERENCES

1. Czarnecki, K. R., Sevier, John R., Jr., and Carmel, Melvin M.: Effects of Fabrication-Type Roughness on Turbulent Skin Friction at Supersonic Speeds. NACA TN 4299, 1958.

2. Czarnecki, K. R., and Monta, William J.: Pressure Distributions and Wave Drag Due to Two-Dimensional Fabrication-Type Surface Roughness on an Ogive Cylinder at Mach Numbers of 1.61 and 2.01. NASA TN D-835, 1961.

3. Brinich, Paul F., and Diaconis, Nick S.: Boundary-Layer Development and Skin Friction at Mach Number 3.05. NACA TN 2742, 1952.

4. Sommer, Simon C., and Short, Barbara J.: Free-Flight Measurements of Turbulent-Boundary-Layer Skin Friction in the Presence of Severe Aerodynamic Heating at Mach Numbers From 2.8 to 7.0. NACA TN 3391, 1955.

TABLE I.- MODEL DESIGNATIONS

Model	Roughness designation	Number of cycles of roughness	Nominal station for profile measurement, x, in.
1	Smooth ogive cylinder		48.00
2	0.020-inch forward steps	18	47.47
3	0.021-inch rearward steps	18	47.35
4	0.021-inch steps with grooves	9	45.76
5	0.019-inch long forward steps	9	44.94
6	0.017-inch transverse creases	24	48.56
7	0.053-inch transverse creases	24	48.50
8	0.053-inch protruding waves	24	47.45 46.65
9	0.020-inch, 45° rearward steps	5 stripes	48.29
10	0.014-inch, 45° creases	6 stripes	47.44

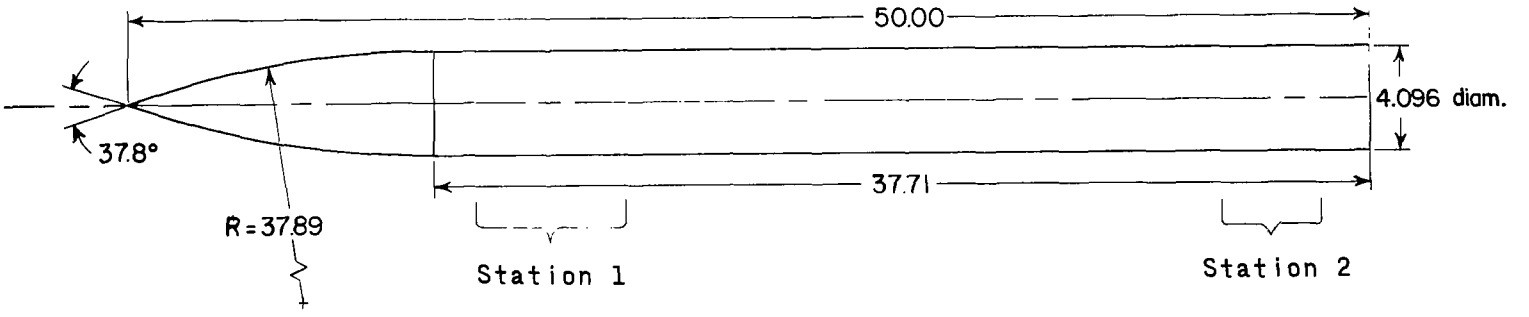

Figure 1.- Sketch of basic model. All dimensions in inches unless otherwise stated.

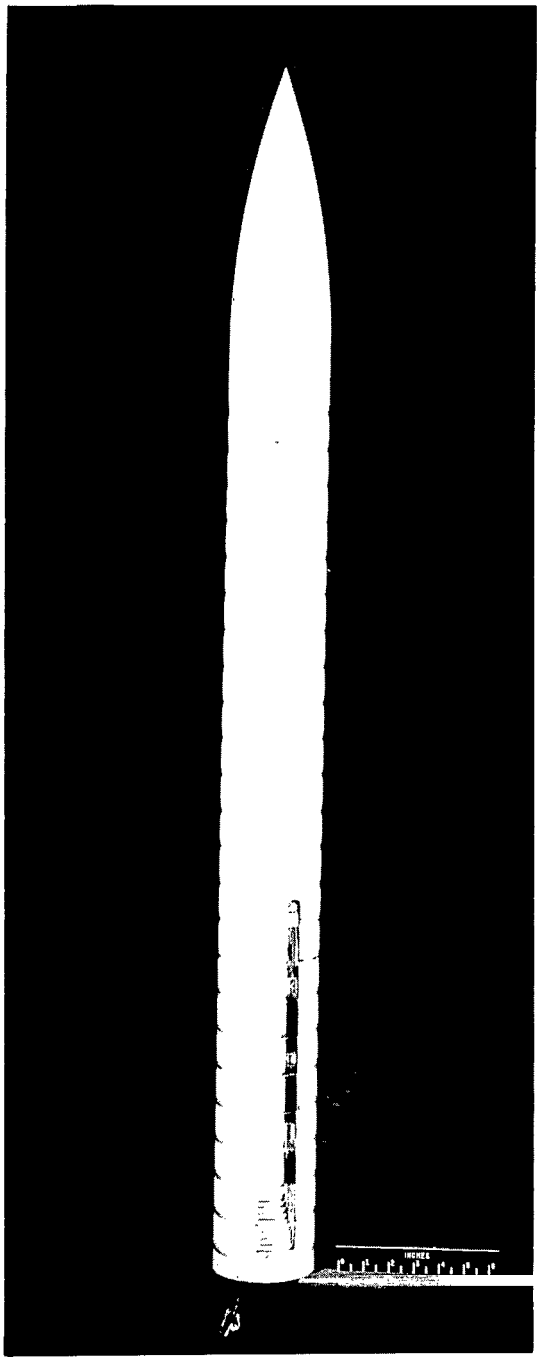

(a) 0.053 transverse creases.

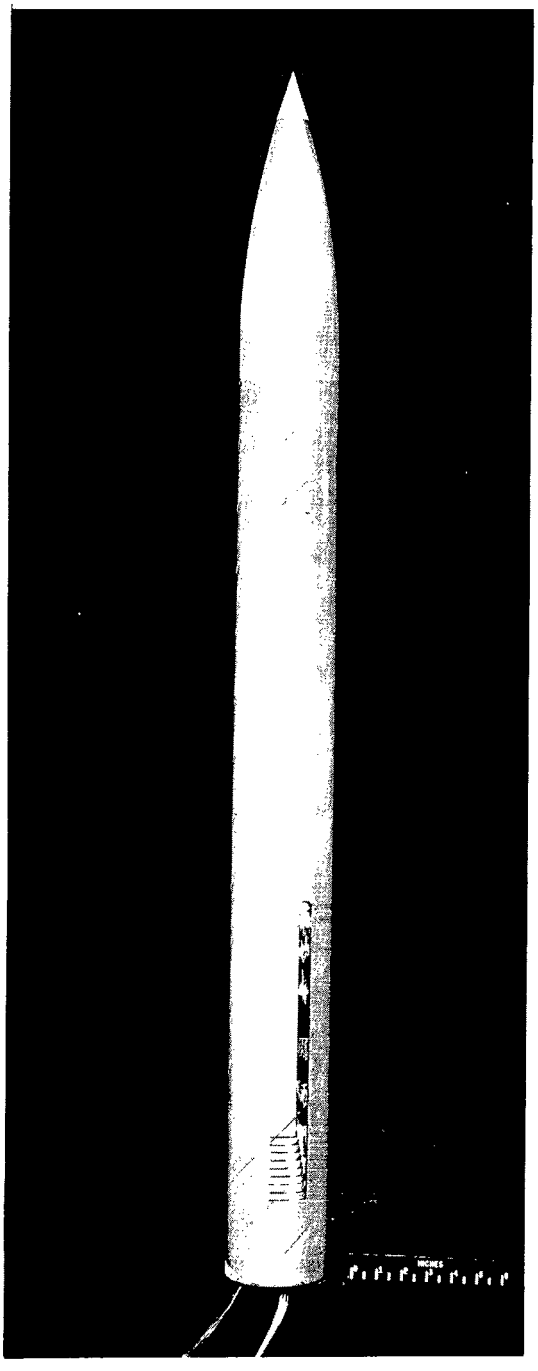

L-61-1039

(b) 0.020, 45° rearward steps.

Figure 2.- Photographs of typical roughness models.

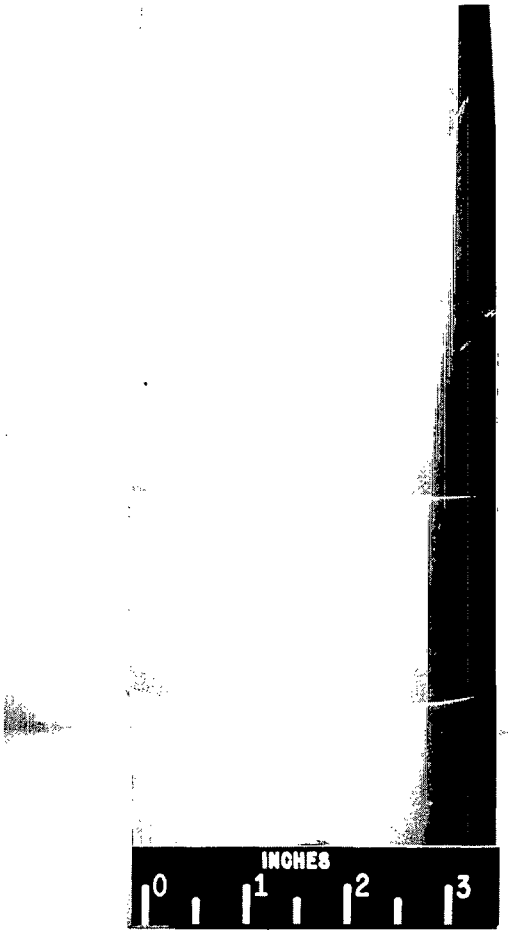

0.020 forward steps

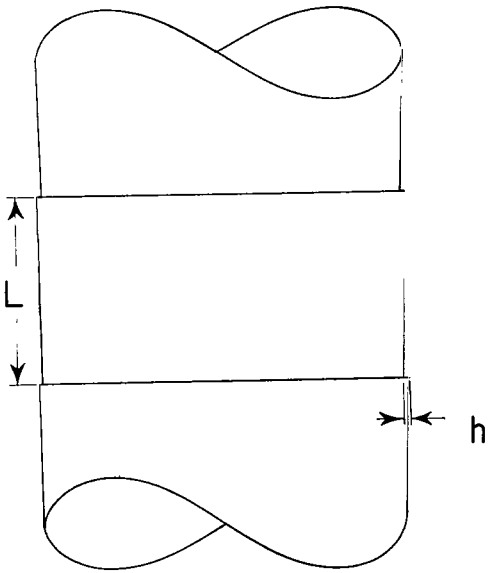

Model	L	h
0.019 long forward steps	4.0	0.019
0.020 forward steps	2.0	0.020

(a) 0.019 long forward or 0.020 forward steps. L-61-1041

Figure 3.- Details of fabrication roughness. All dimensions in inches unless otherwise stated.

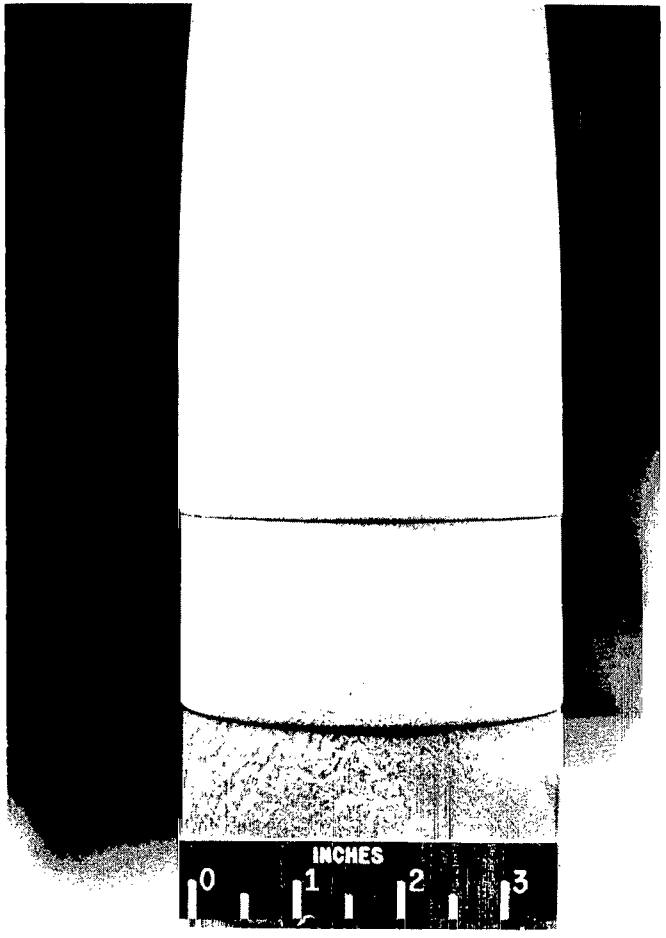

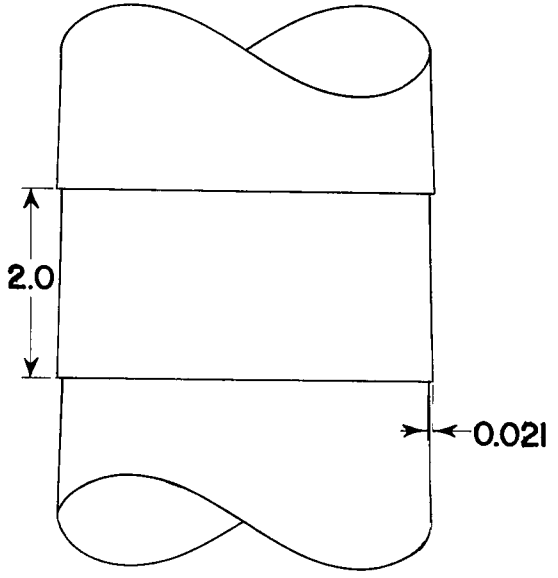

(b) 0.021 rearward steps. L-61-1042

Figure 3.- Continued.

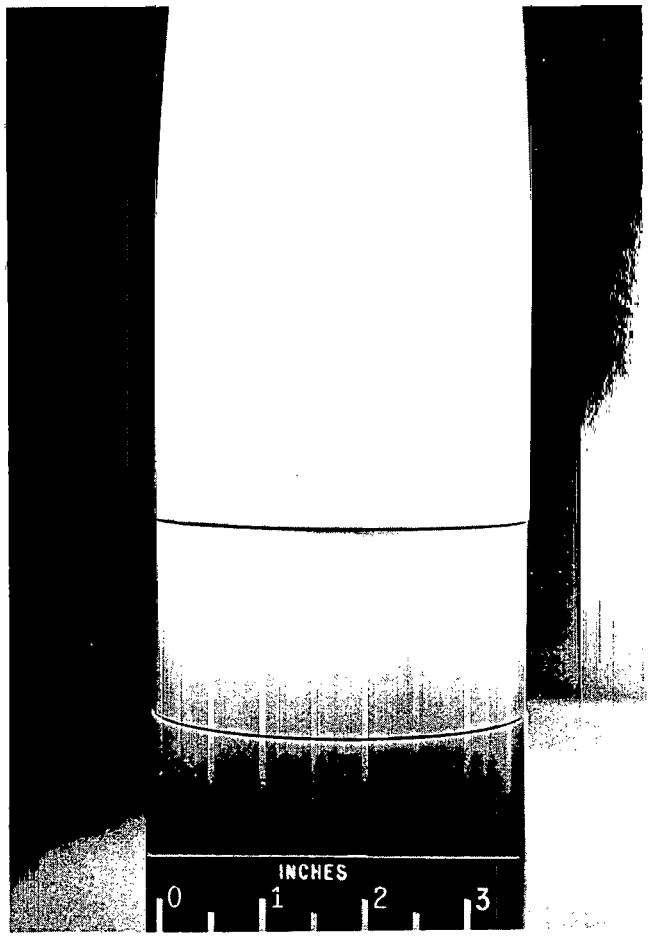

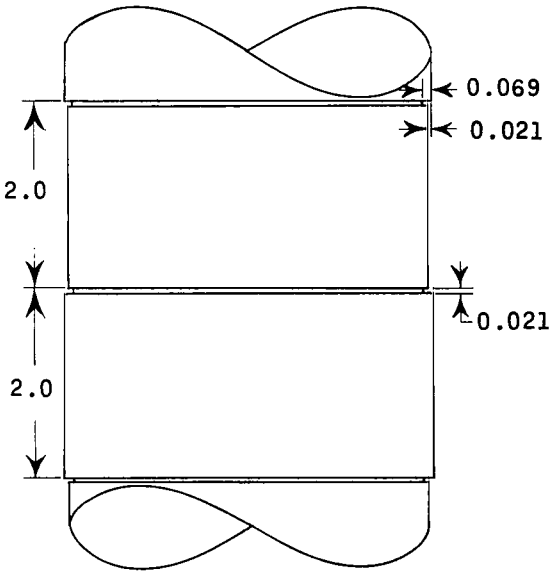

(c) 0.021 steps with grooves. L-61-1040

Figure 3.- Continued.

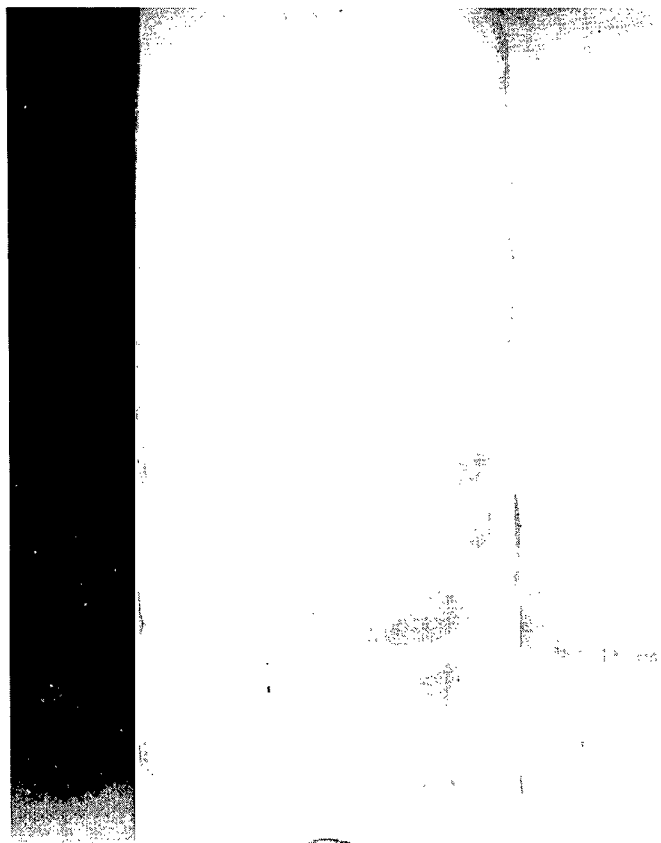

0.053 transverse creases

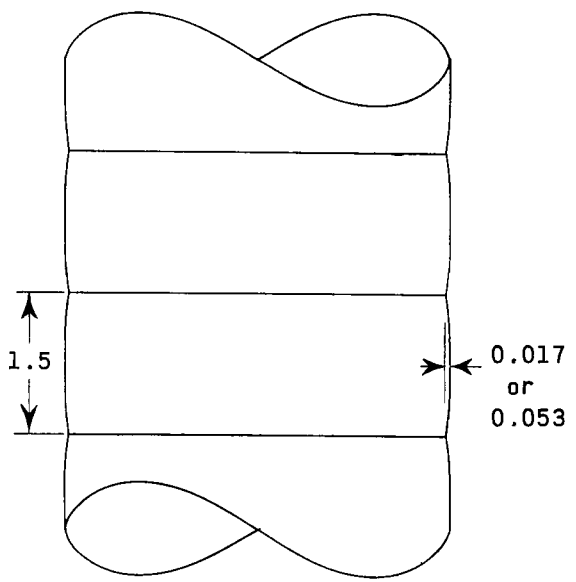

(d) 0.017 and 0.053 transverse creases. L-61-1044

Figure 3.- Continued.

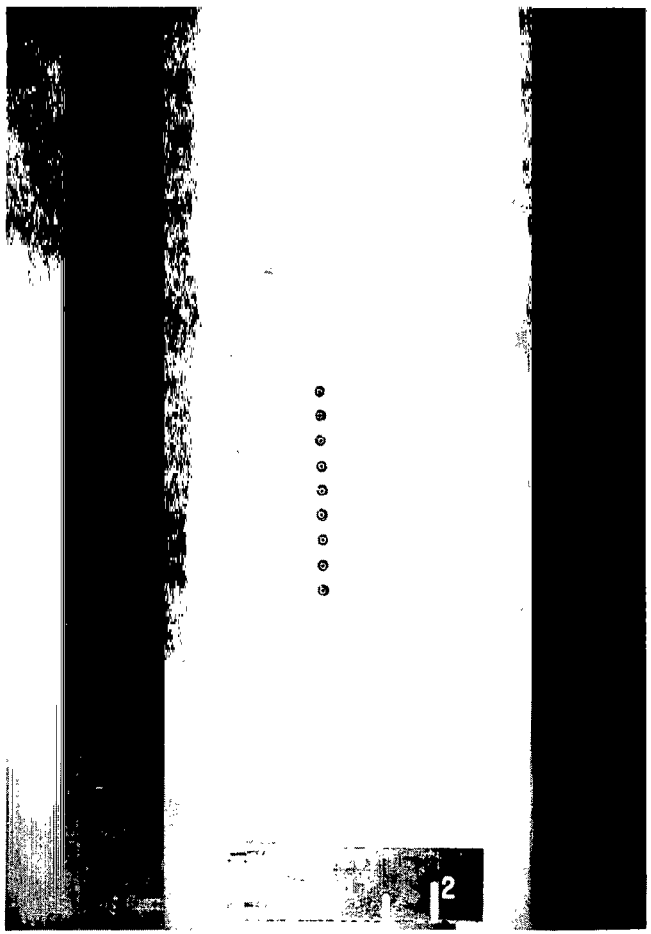

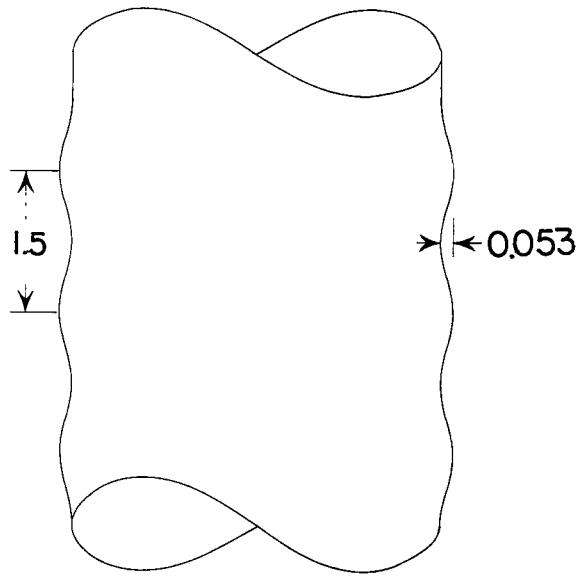

0.053 protruding waves

(e) 0.053 protruding waves. L-61-1043

Figure 3.- Continued.

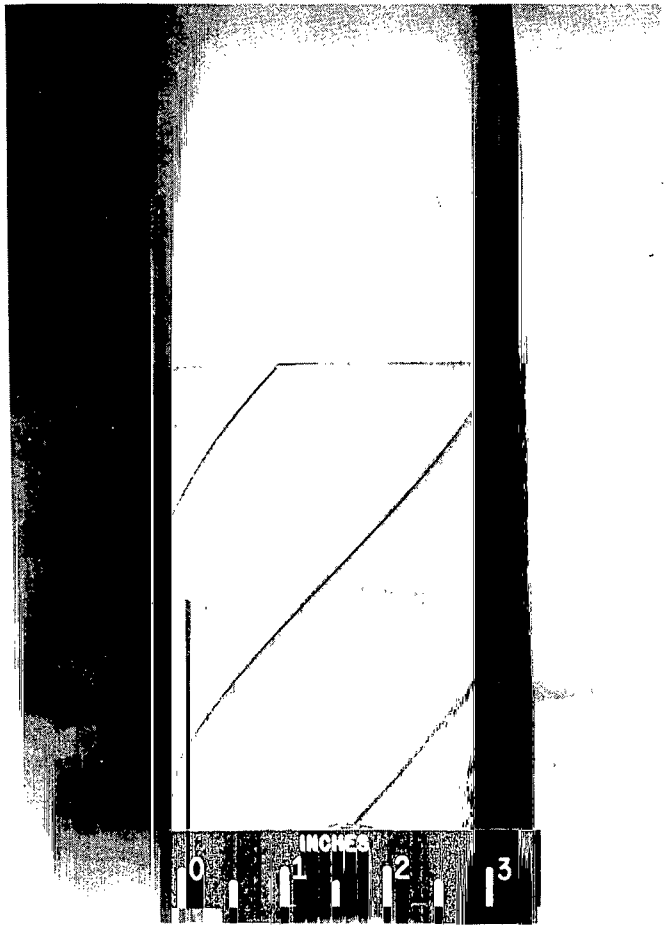

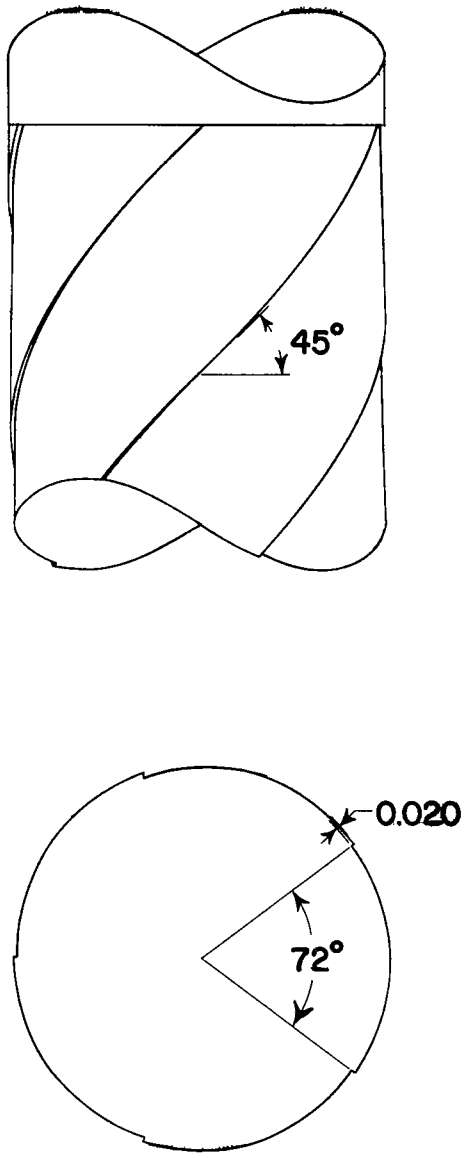

(f) 0.020, 45° rearward steps. L-61-1045

Figure 3.- Continued.

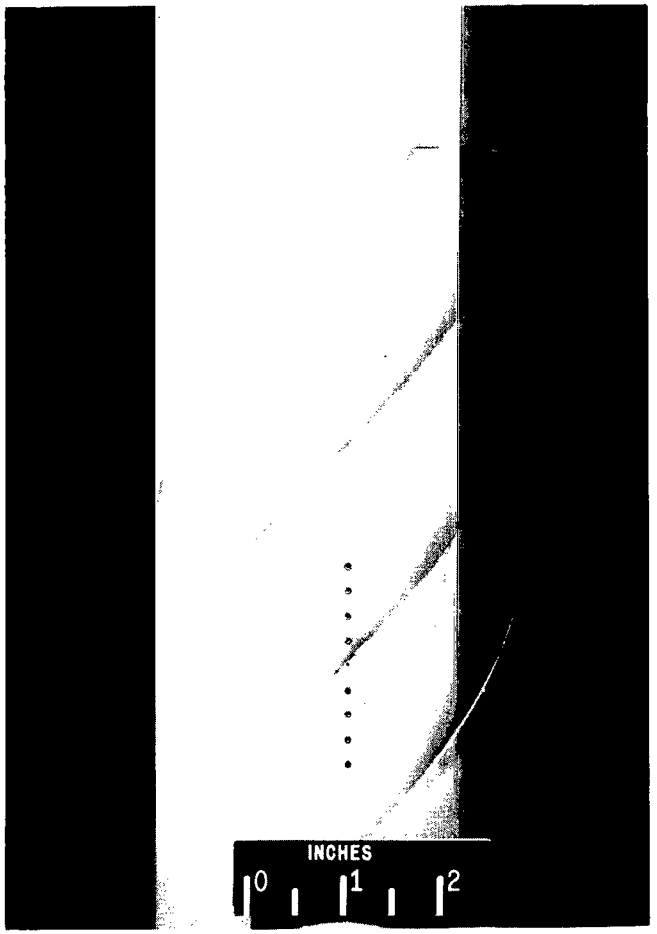

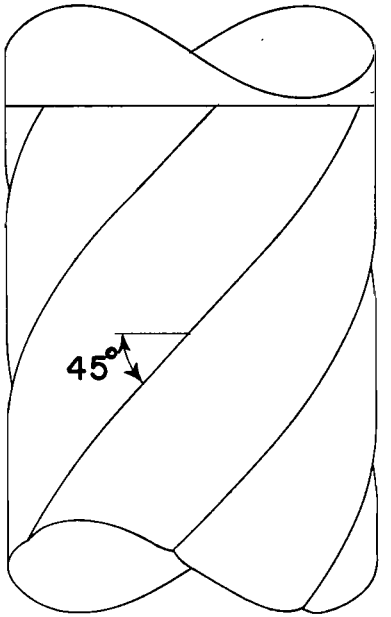

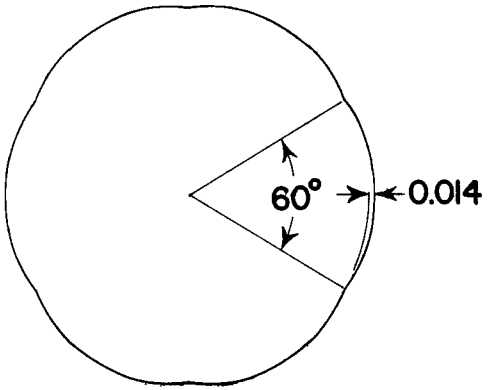

(g) 0.014, 45° creases. L-61-1046

Figure 3.- Concluded.

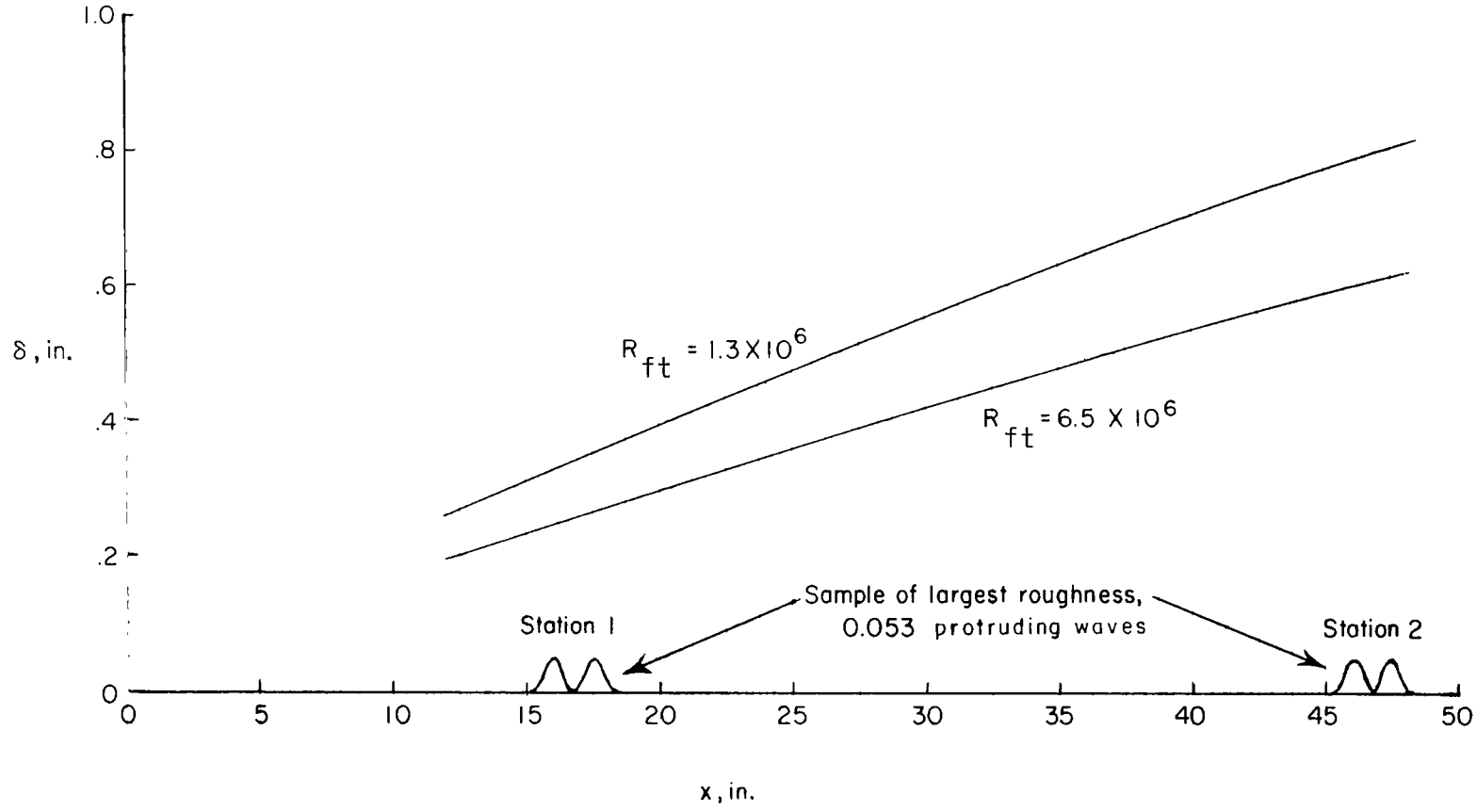

Figure 4.- Comparison of estimated boundary-layer thickness δ with the highest roughness configuration. $M_\infty = 1.61$.

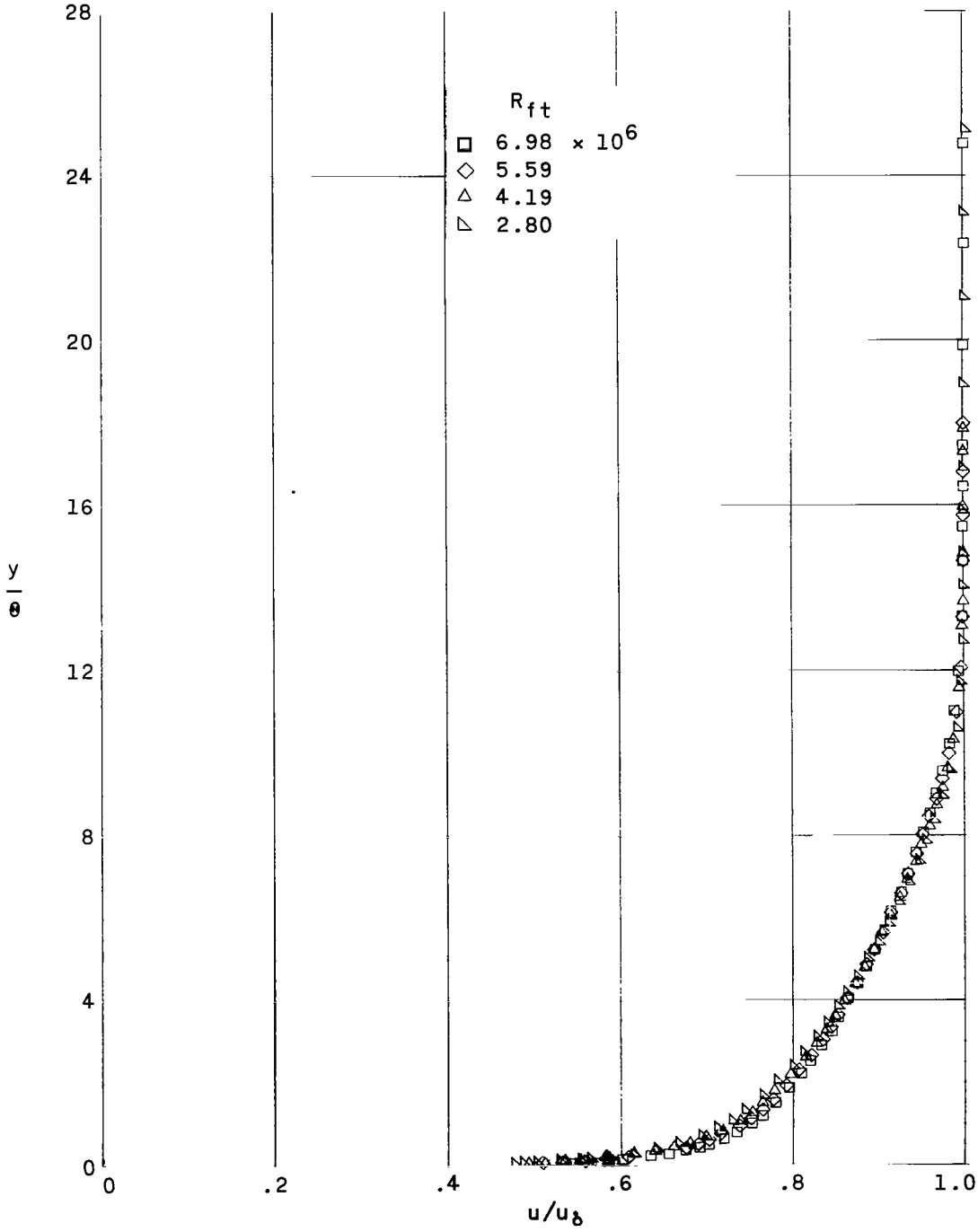

(a) Smooth ogive cylinder.

Figure 5.- Typical nondimensional boundary-layer velocity profiles. M_∞ = 1.61.

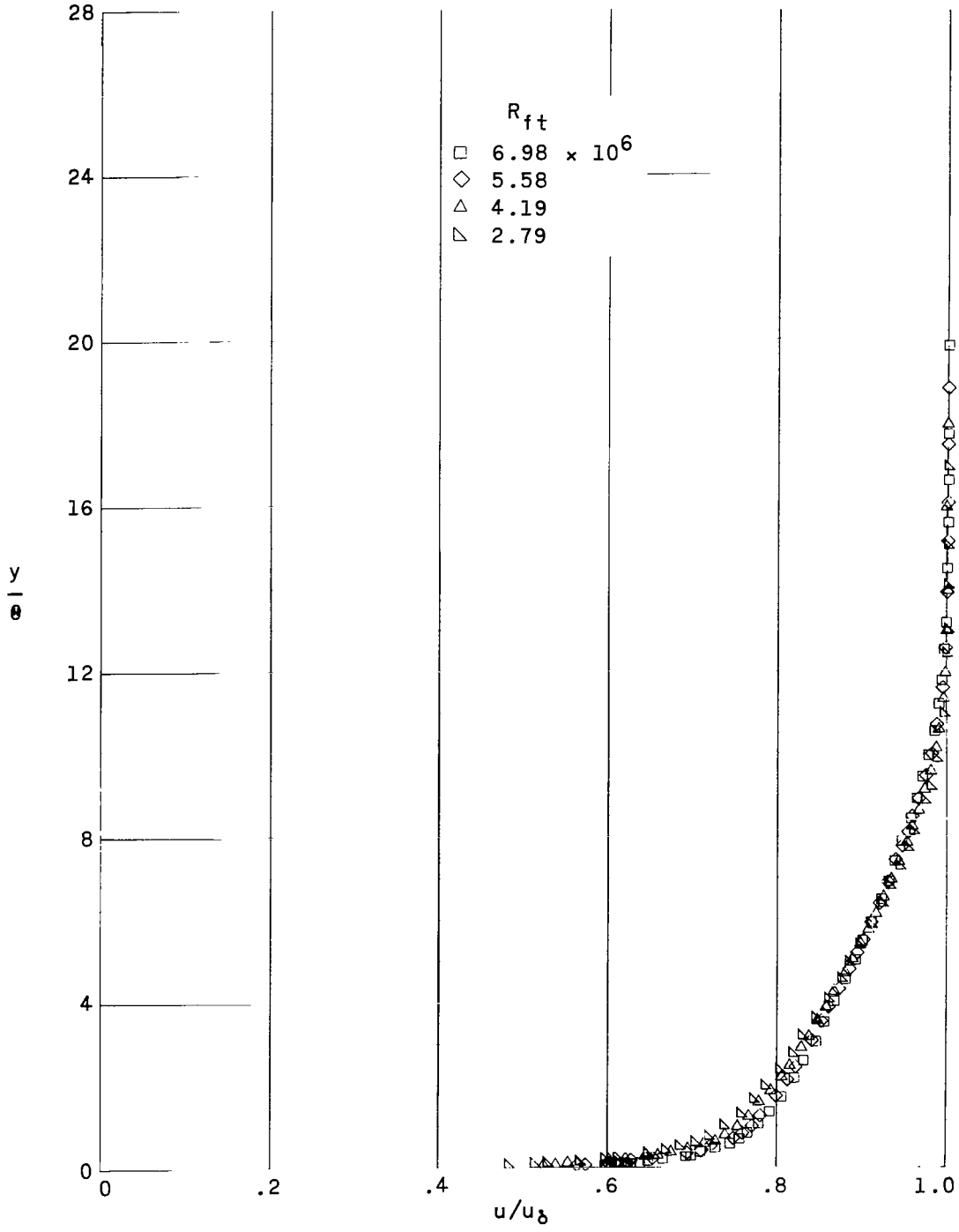

(b) 0.020 forward steps.

Figure 5.- Continued.

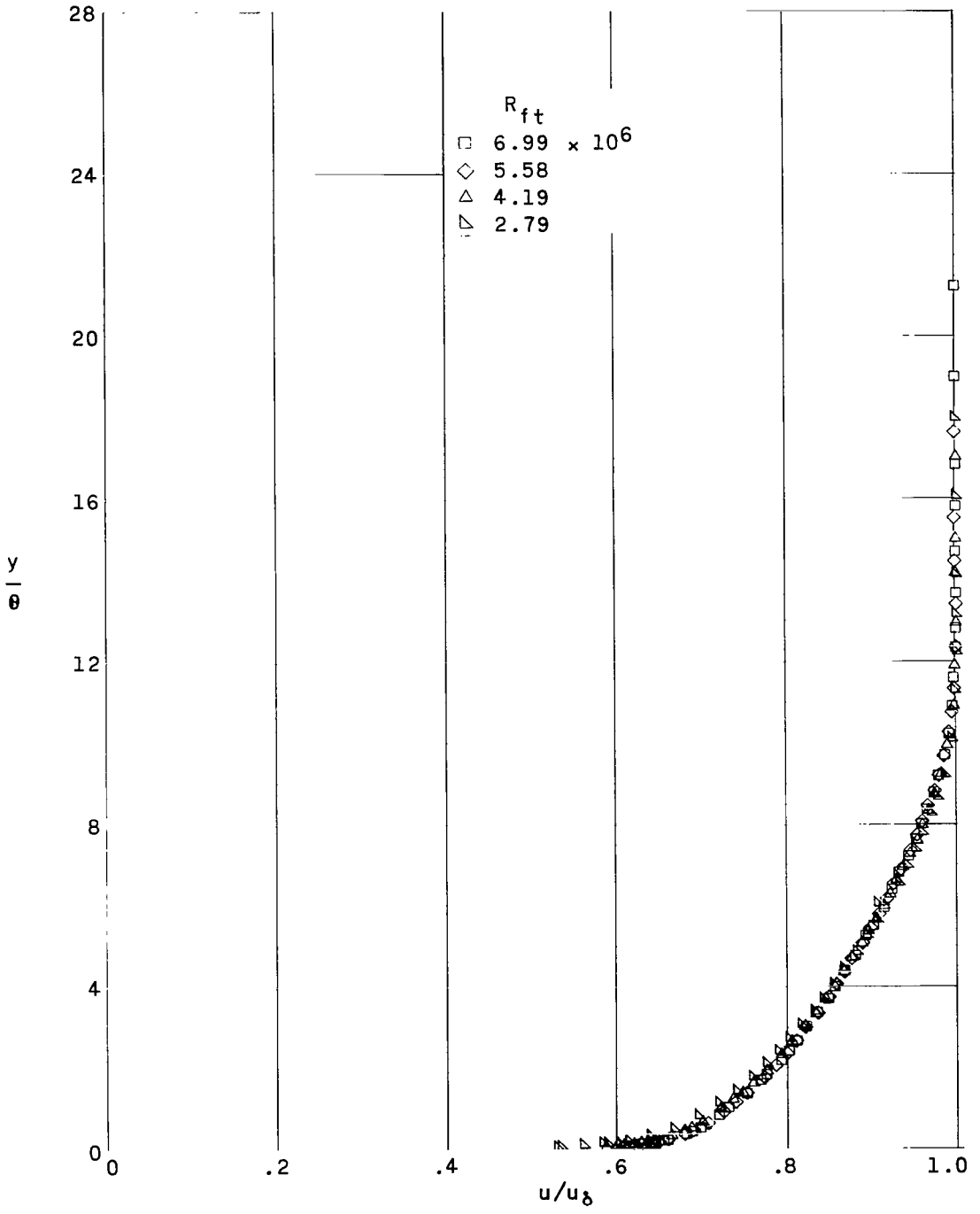

(c) 0.021 steps with grooves.

Figure 5.- Continued.

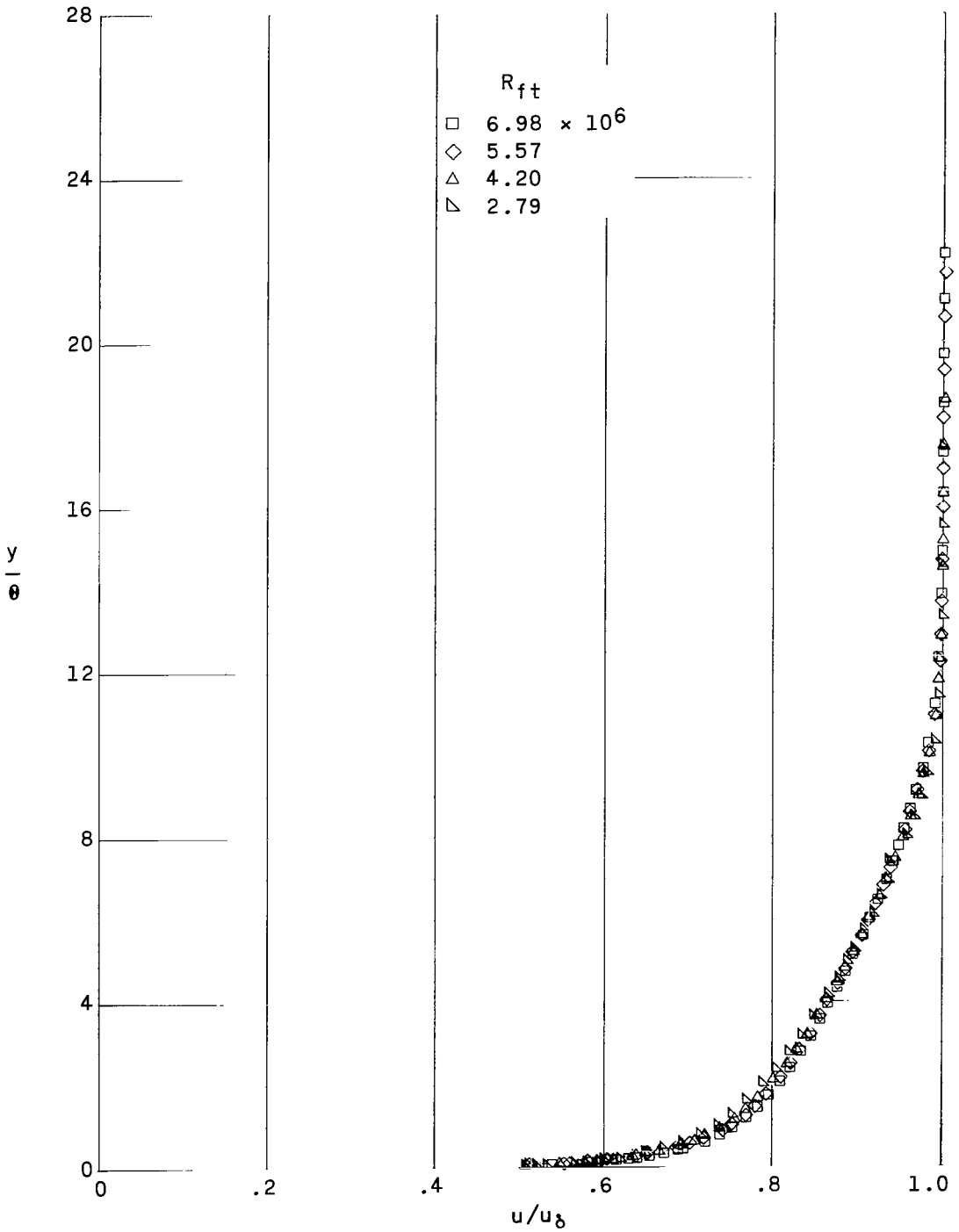

(d) 0.020, 45° rearward steps.

Figure 5.- Continued.

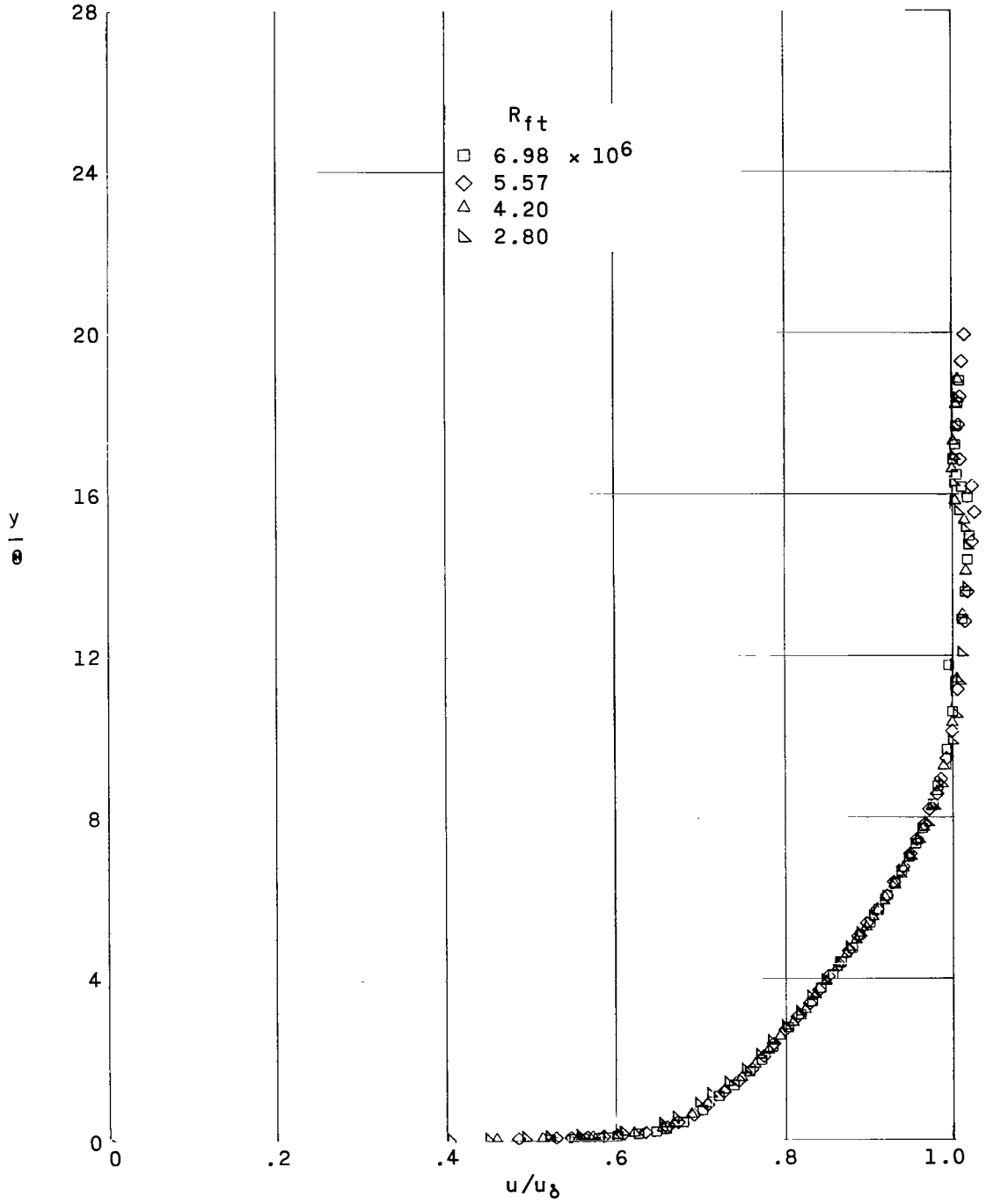

(e) 0.53 transverse creases.

Figure 5.- Continued.

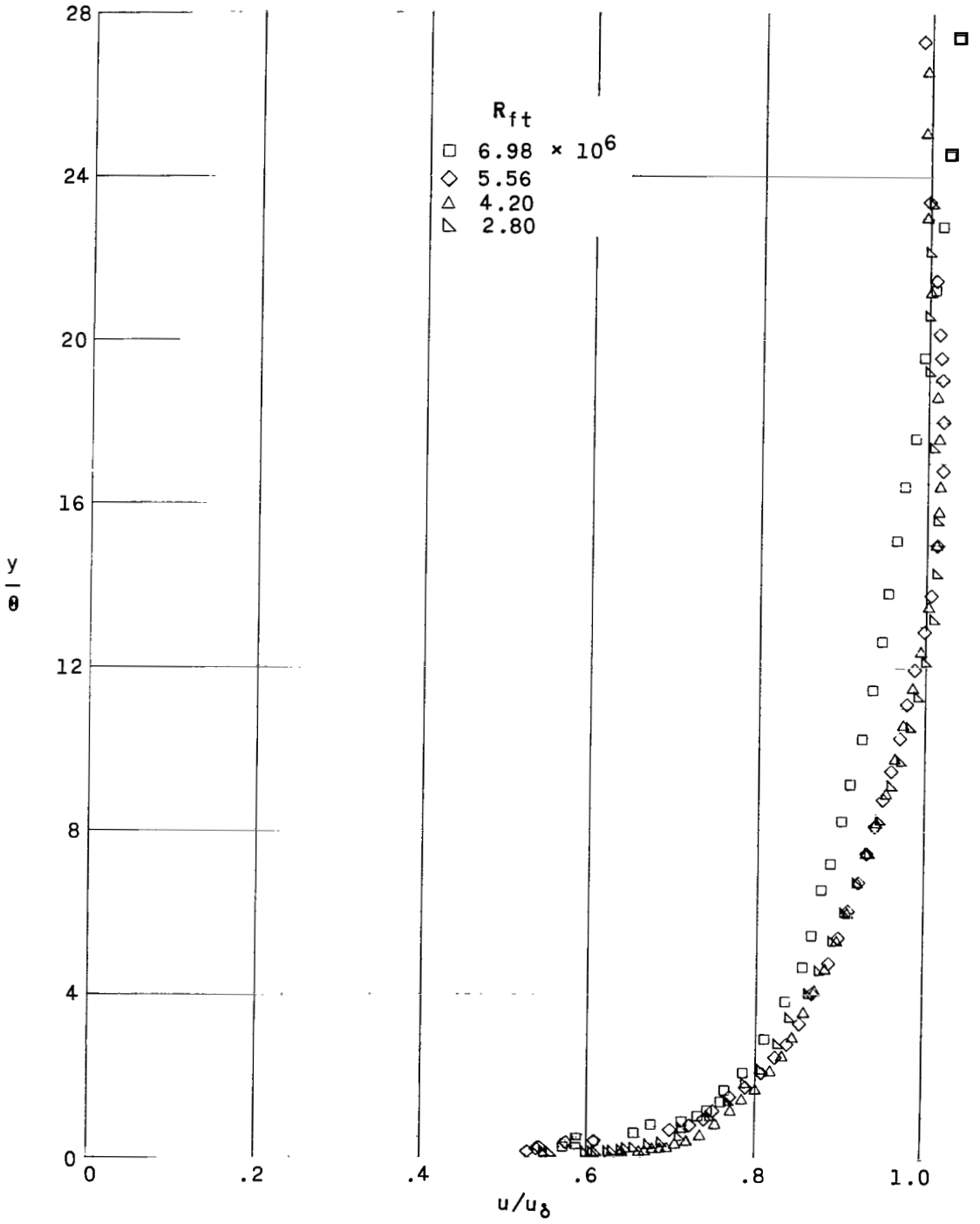

(f) 0.053 protruding waves.

Figure 5.- Concluded.

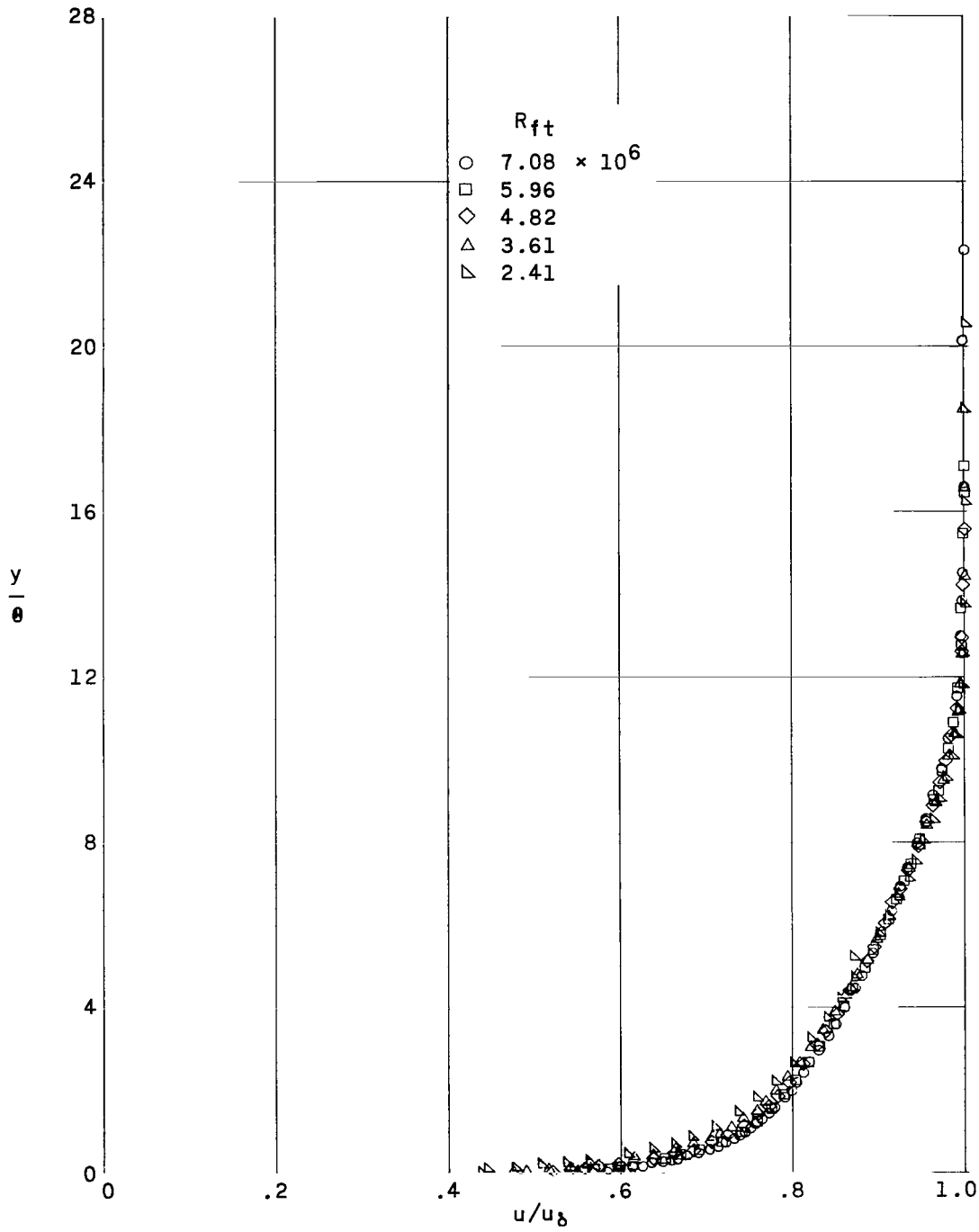

(a) Smooth ogive cylinder.

Figure 6.- Typical nondimensional boundary-layer velocity profiles. M_∞= 2.01.

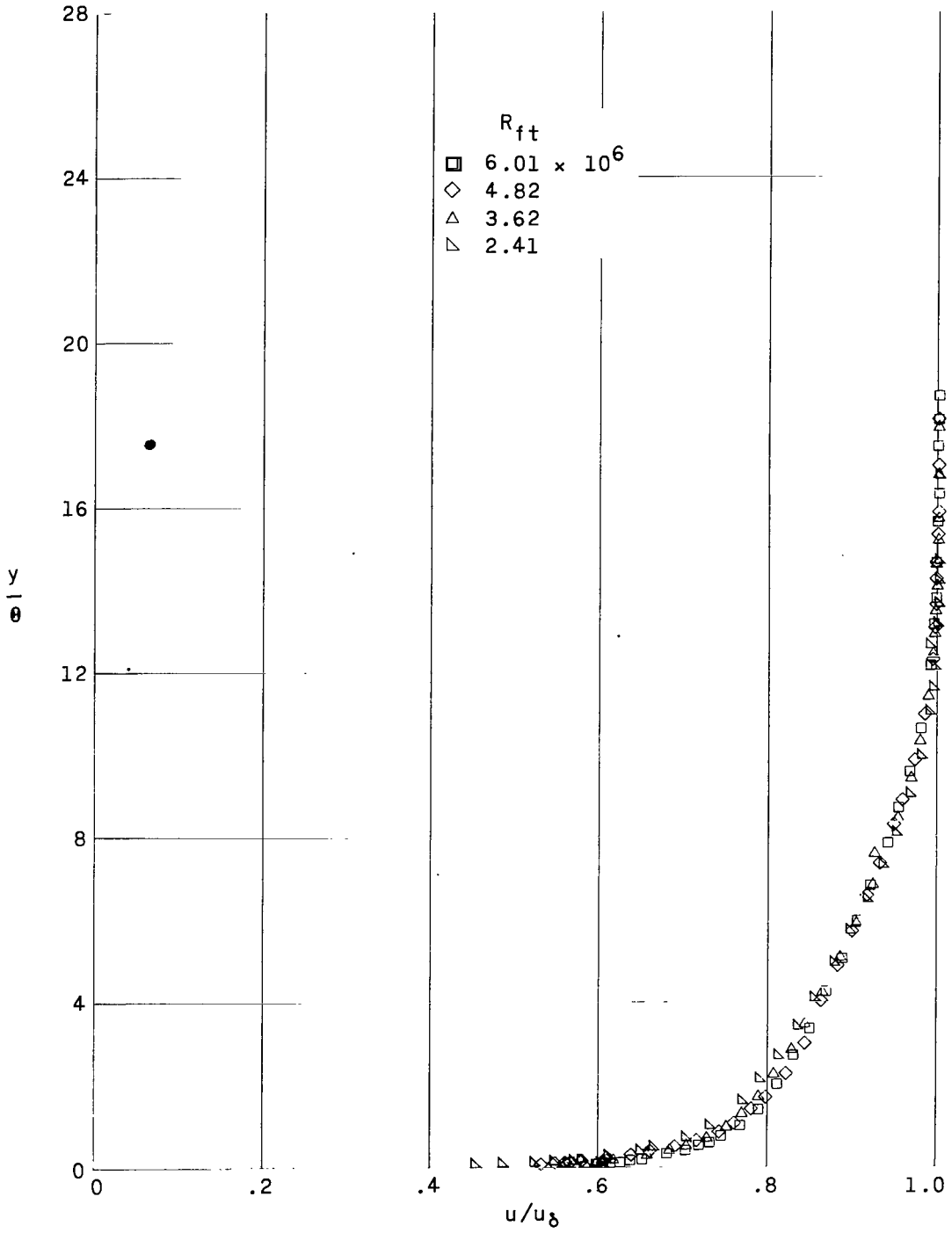

(b) 0.020 forward steps.

Figure 6.- Continued.

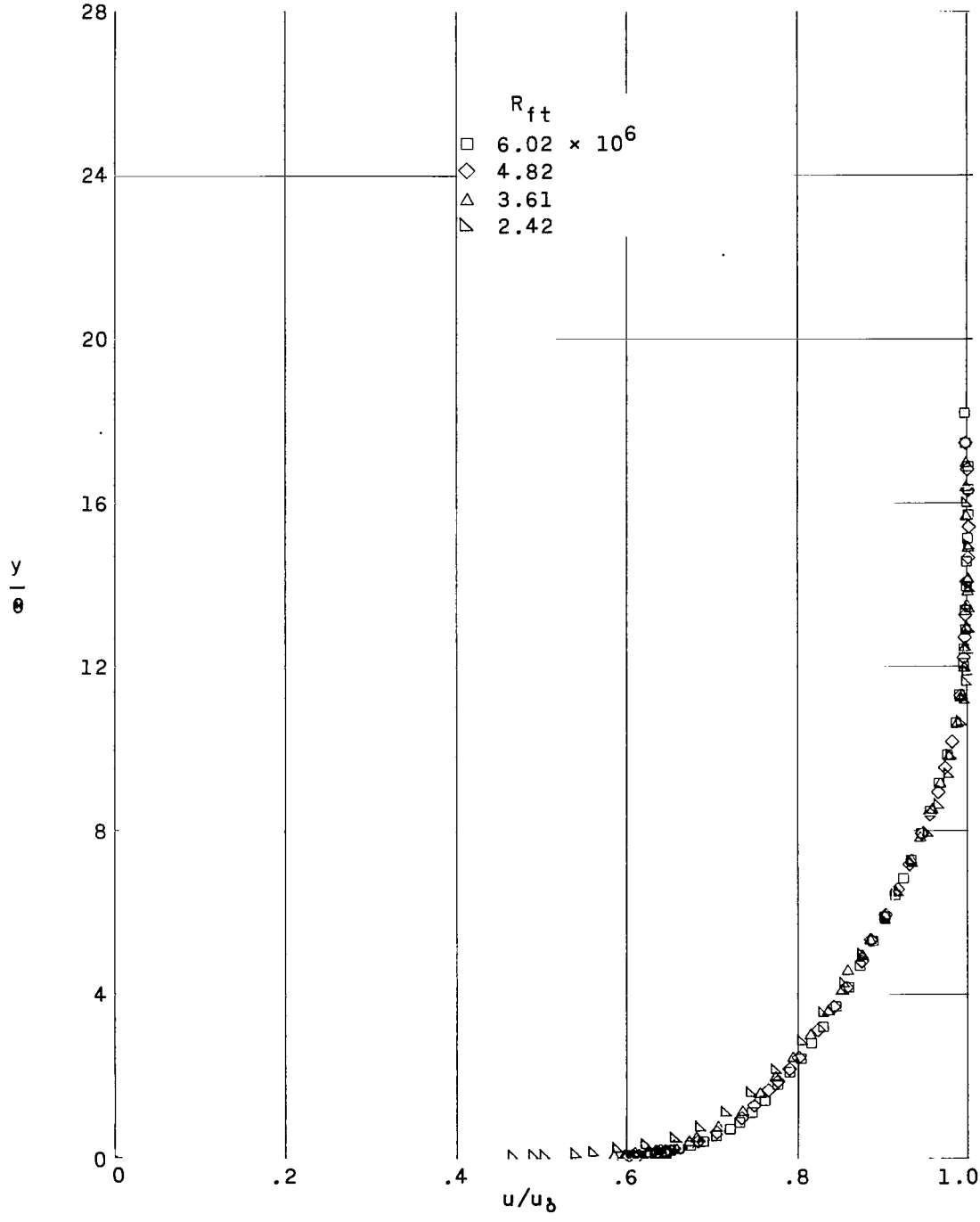

(c) 0.021 steps with grooves.

Figure 6.- Continued.

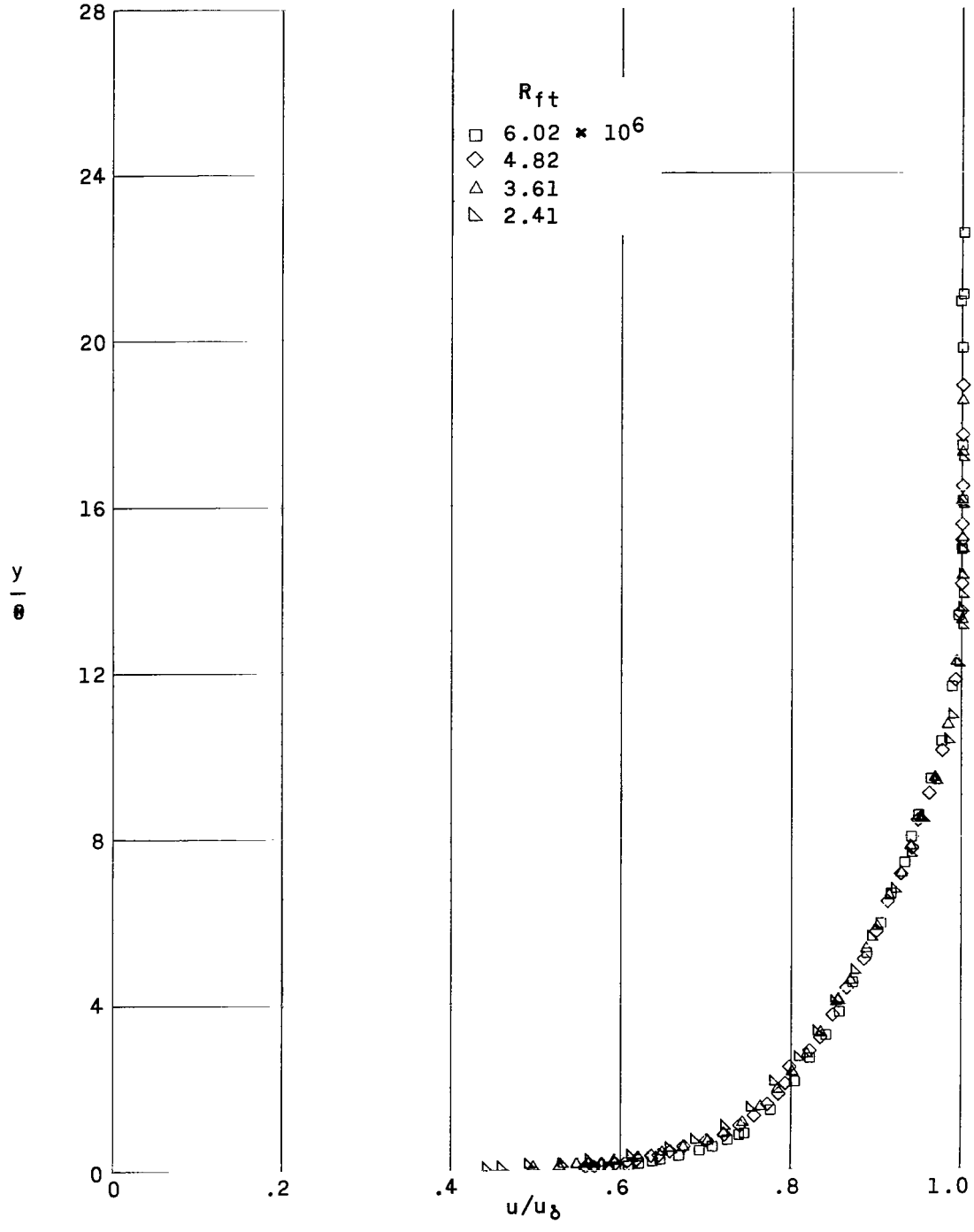

(d) 0.020, 45° rearward steps.

Figure 6.- Continued.

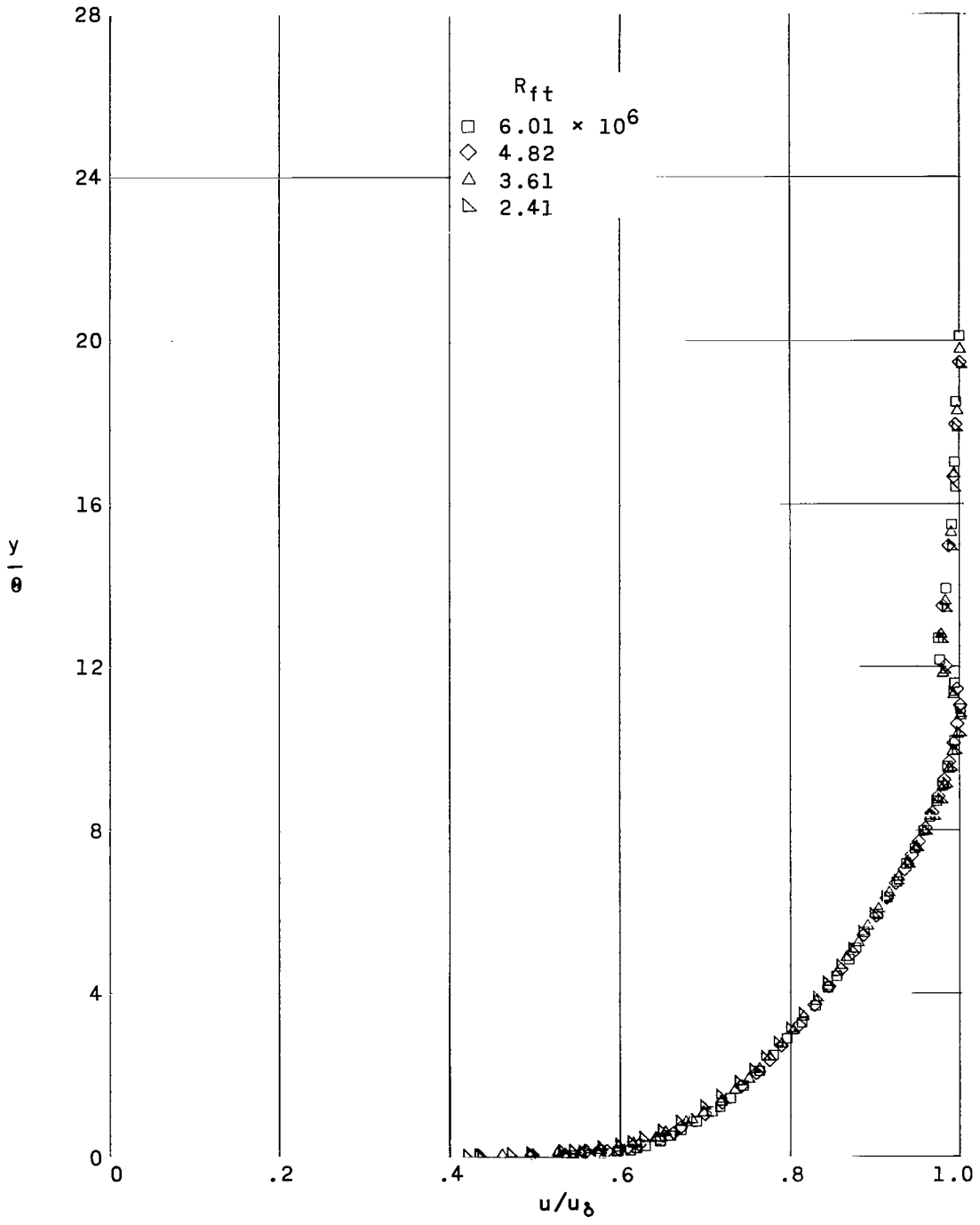

(e) 0.053 transverse creases.

Figure 6.- Continued.

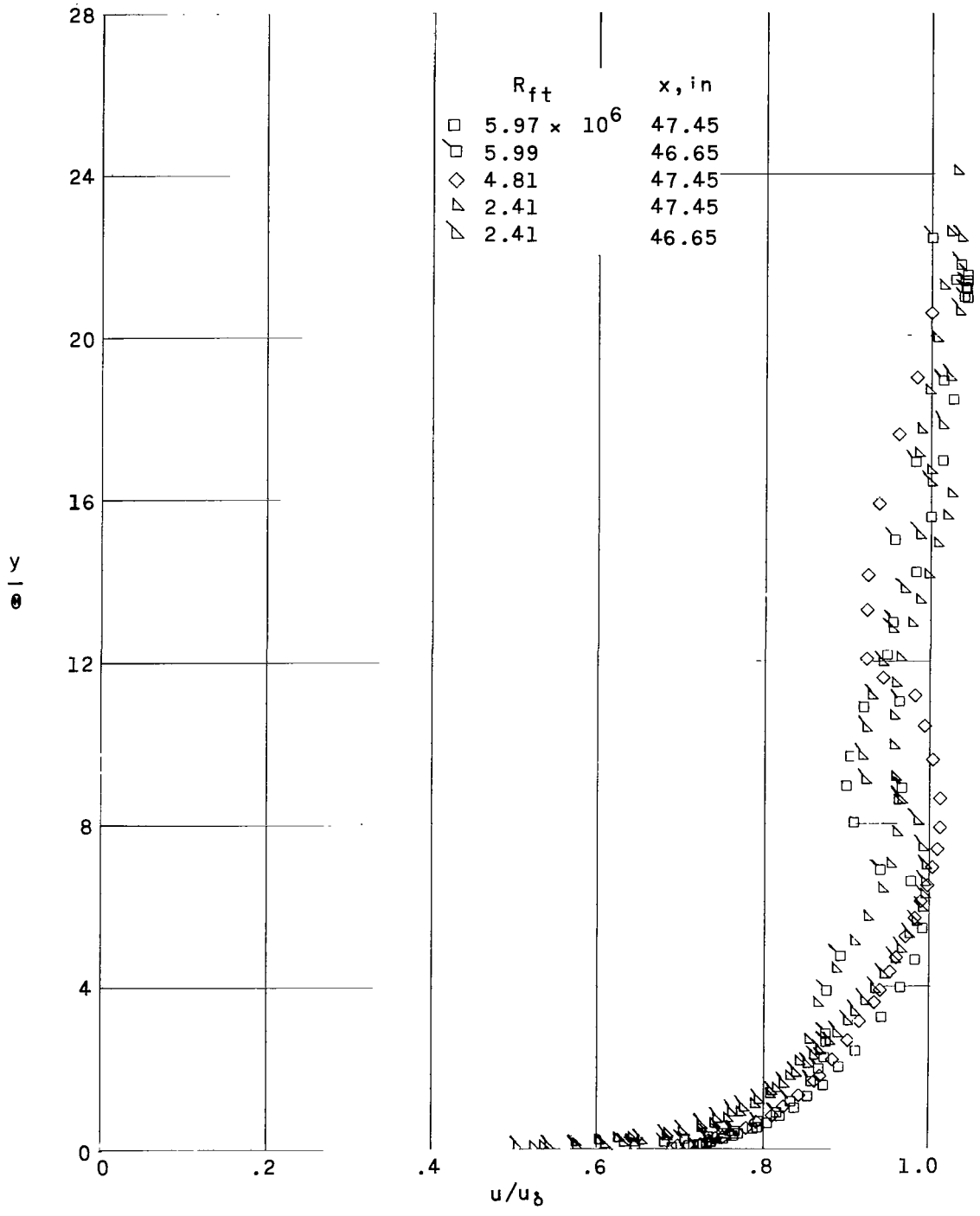

(f) 0.053 protruding waves.

Figure 6.- Concluded.

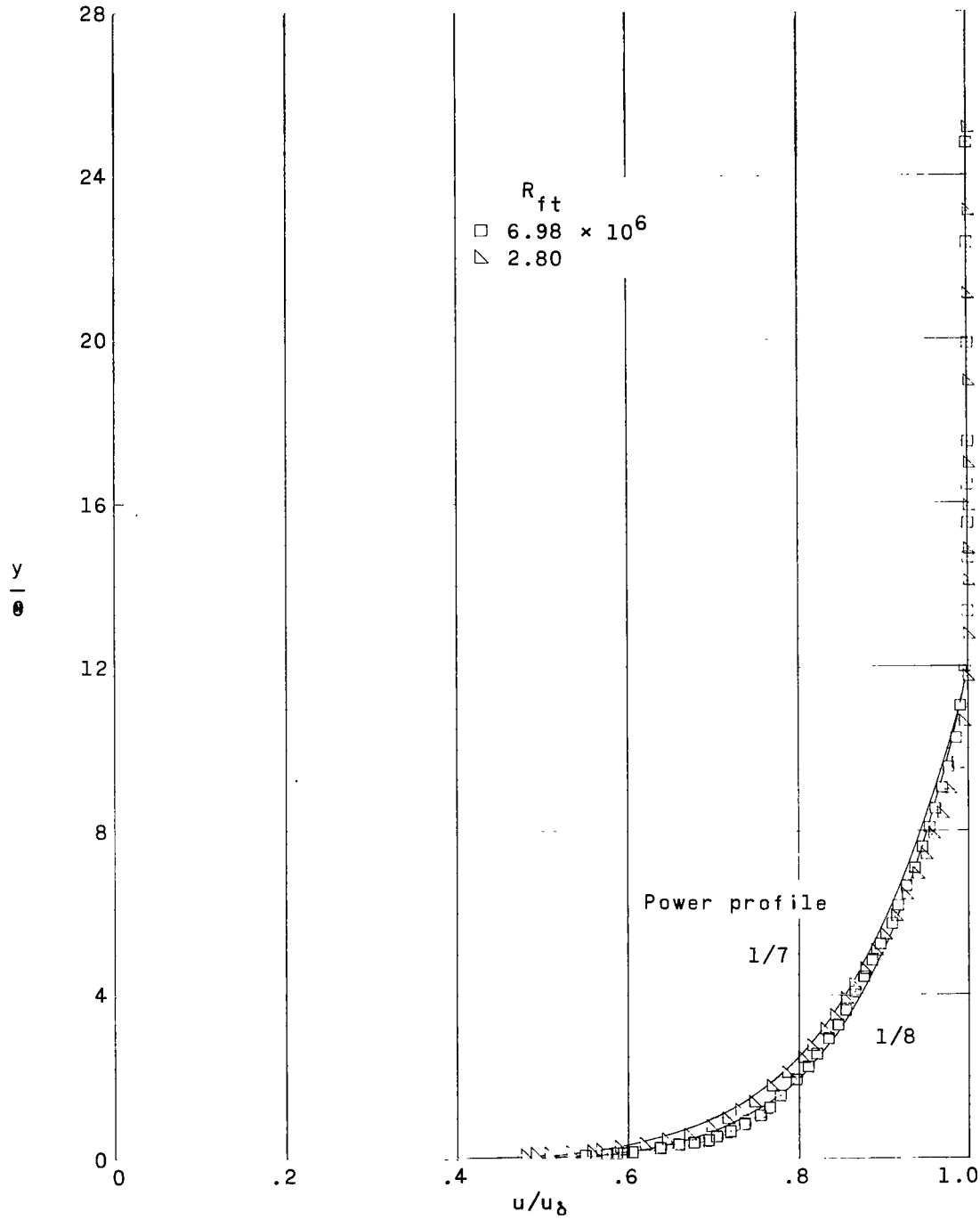

Figure 7.- Comparison of experimental boundary-layer velocity profiles with 1/7- and 1/8-power velocity distributions. $M_\infty = 1.61$.

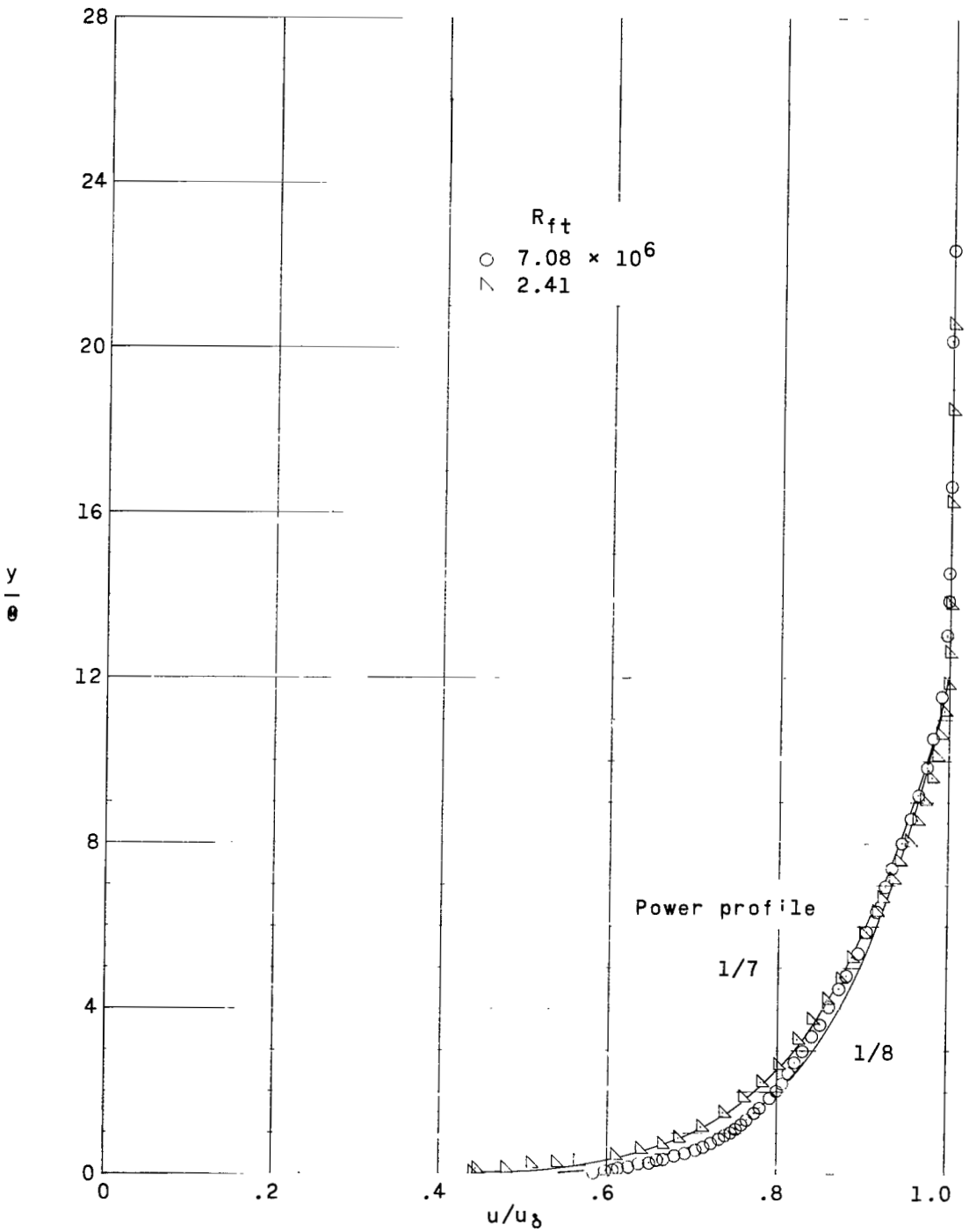

Figure 8.- Comparison of experimental boundary-layer velocity profiles with 1/7- and 1/8-power velocity distributions. $M_\infty = 2.01$.

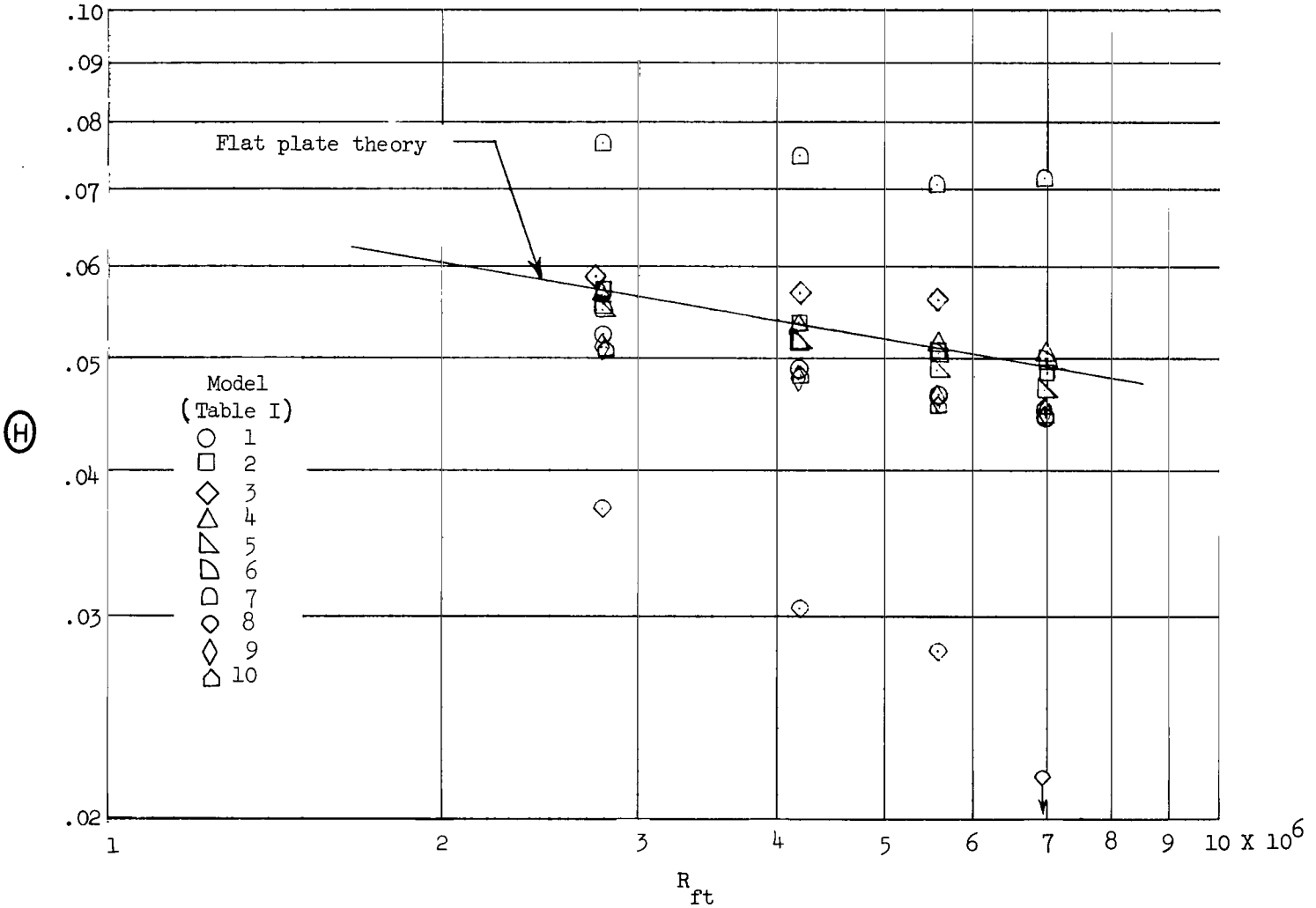

Figure 9.- Effect of surface roughness on boundary-layer momentum thickness. M_∞ = 1.61; x = 44.94 to 48.56 inches.

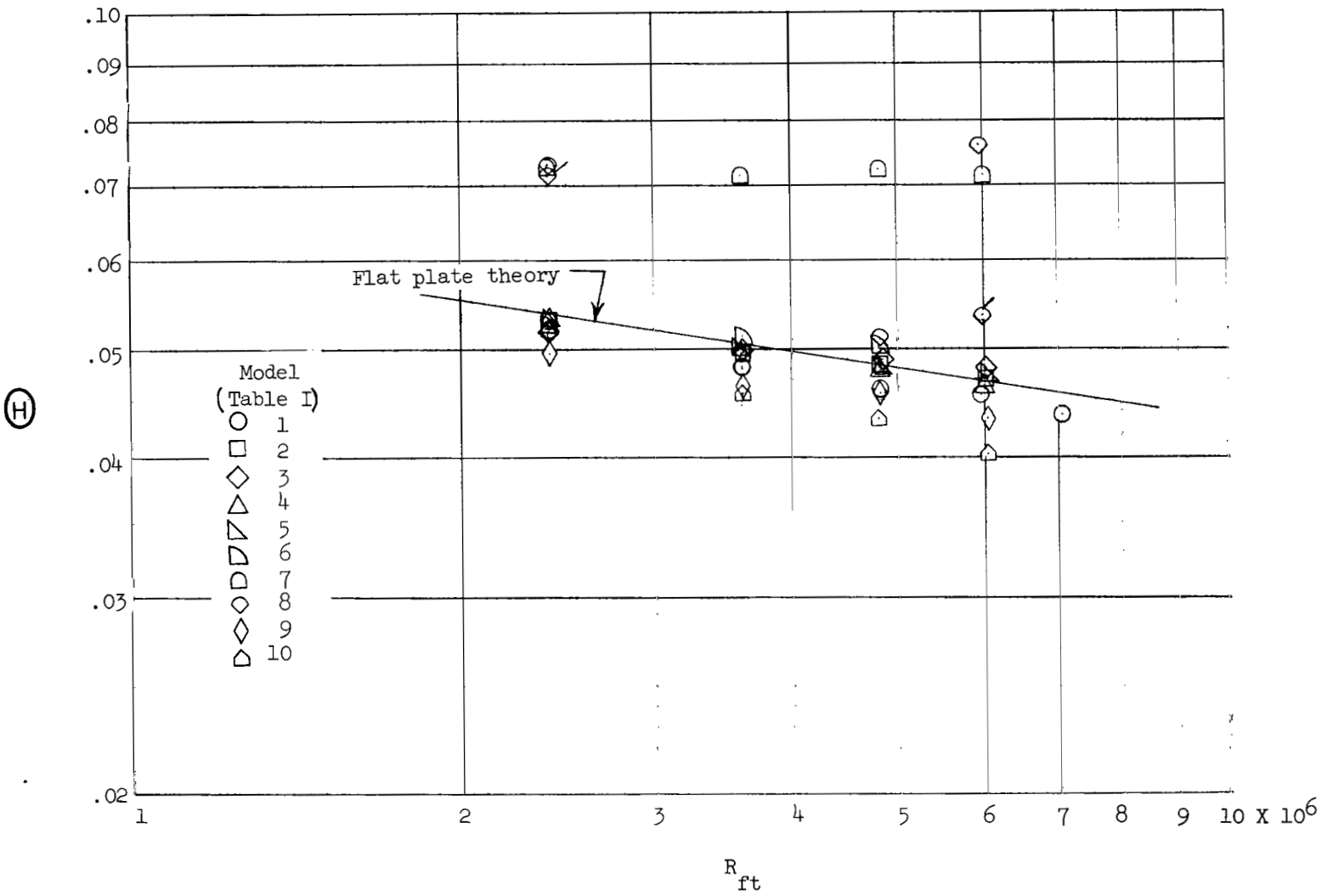

Figure 10.- Effect of surface roughness on boundary-layer momentum thickness. M_∞ = 2.01; x = 44.94 to 48.56 inches. Flagged symbol indicates data taken at alternate survey station.

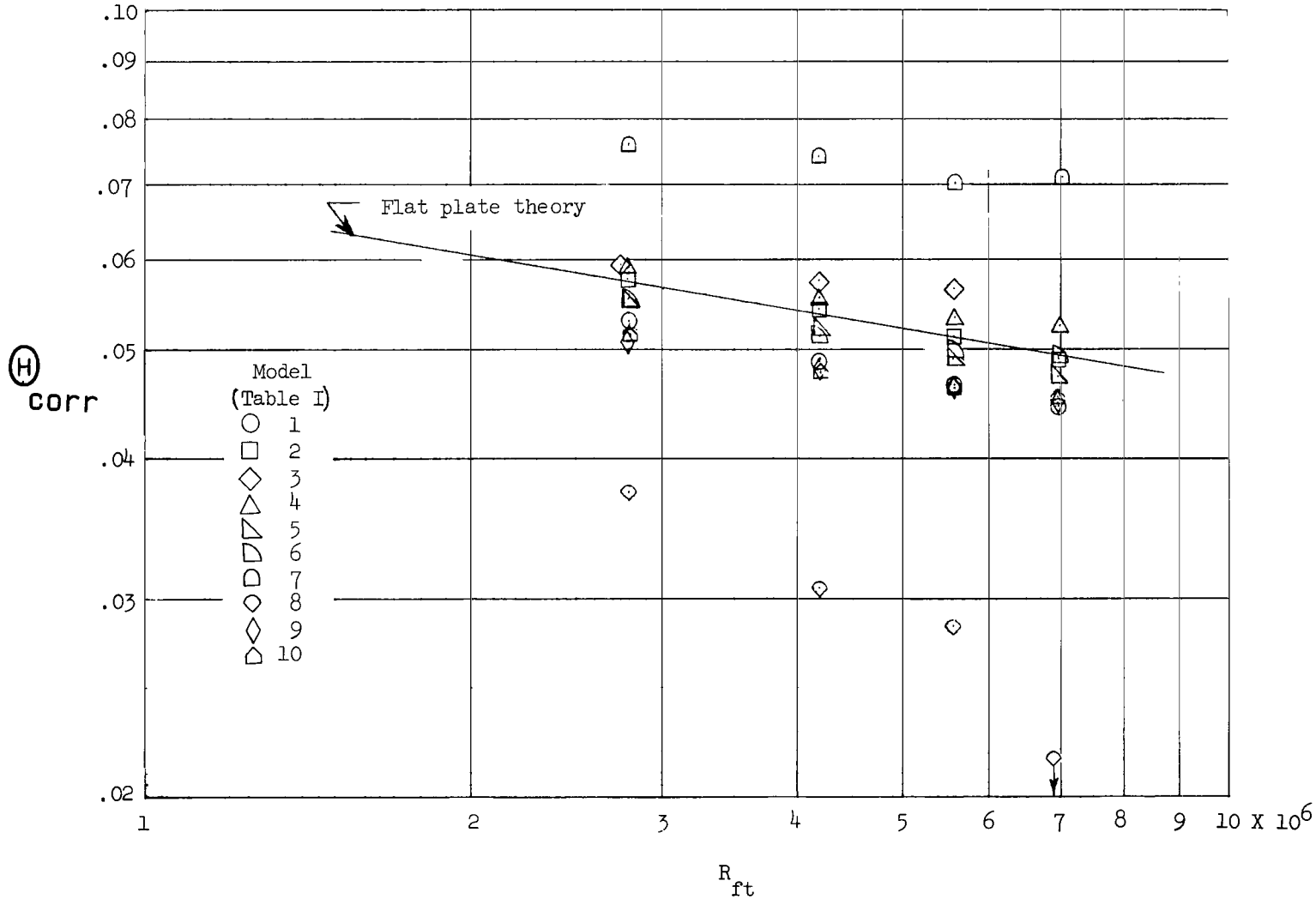

Figure 11.- Effect of surface roughness on corrected boundary-layer momentum thickness. $M_\infty = 1.61$; x = 48 inches.

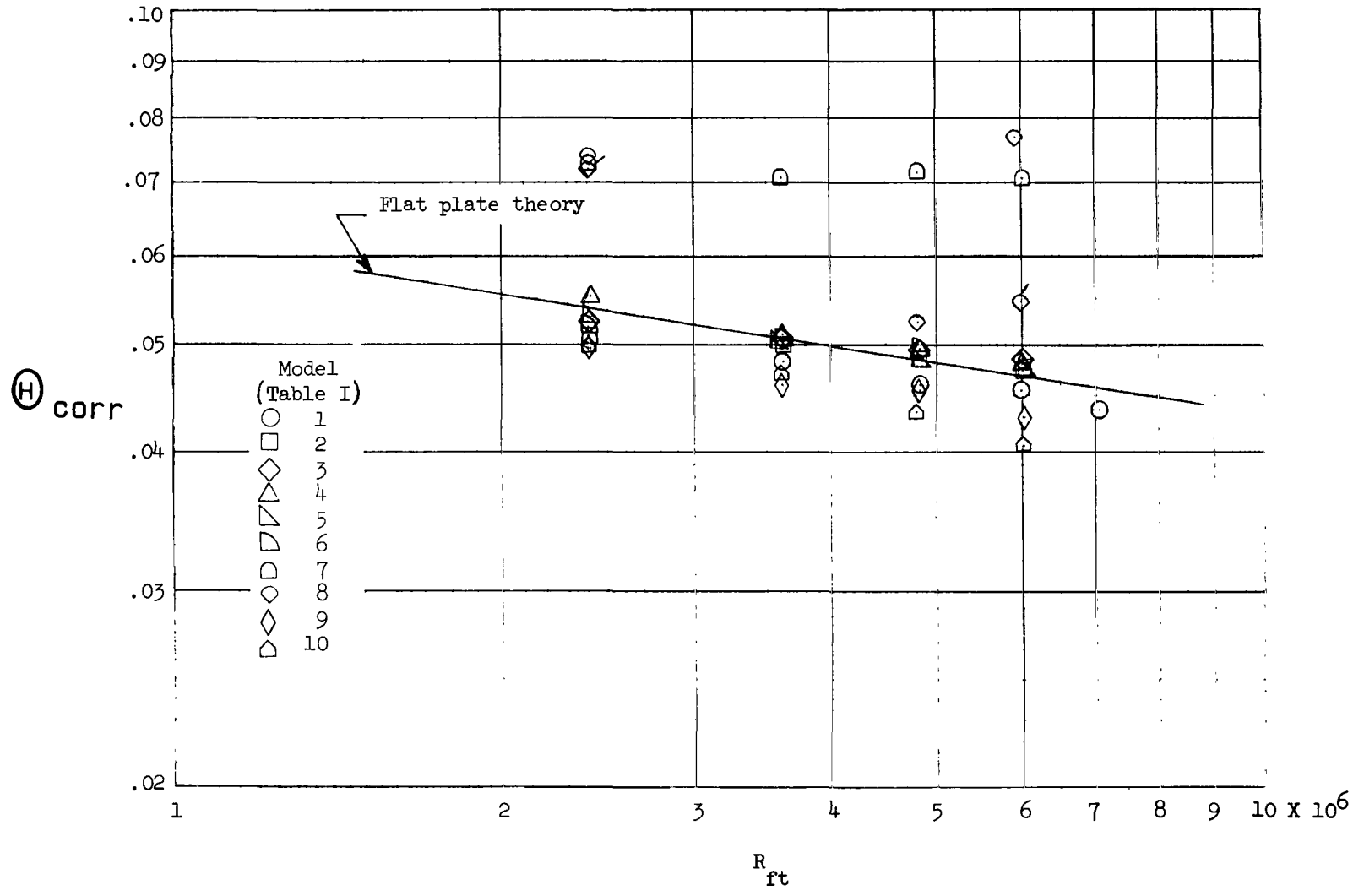

Figure 12.- Effect of surface roughness on corrected boundary-layer momentum thickness. M_∞ = 2.01; x = 48 inches. Flagged symbol indicates data taken at alternate survey station.

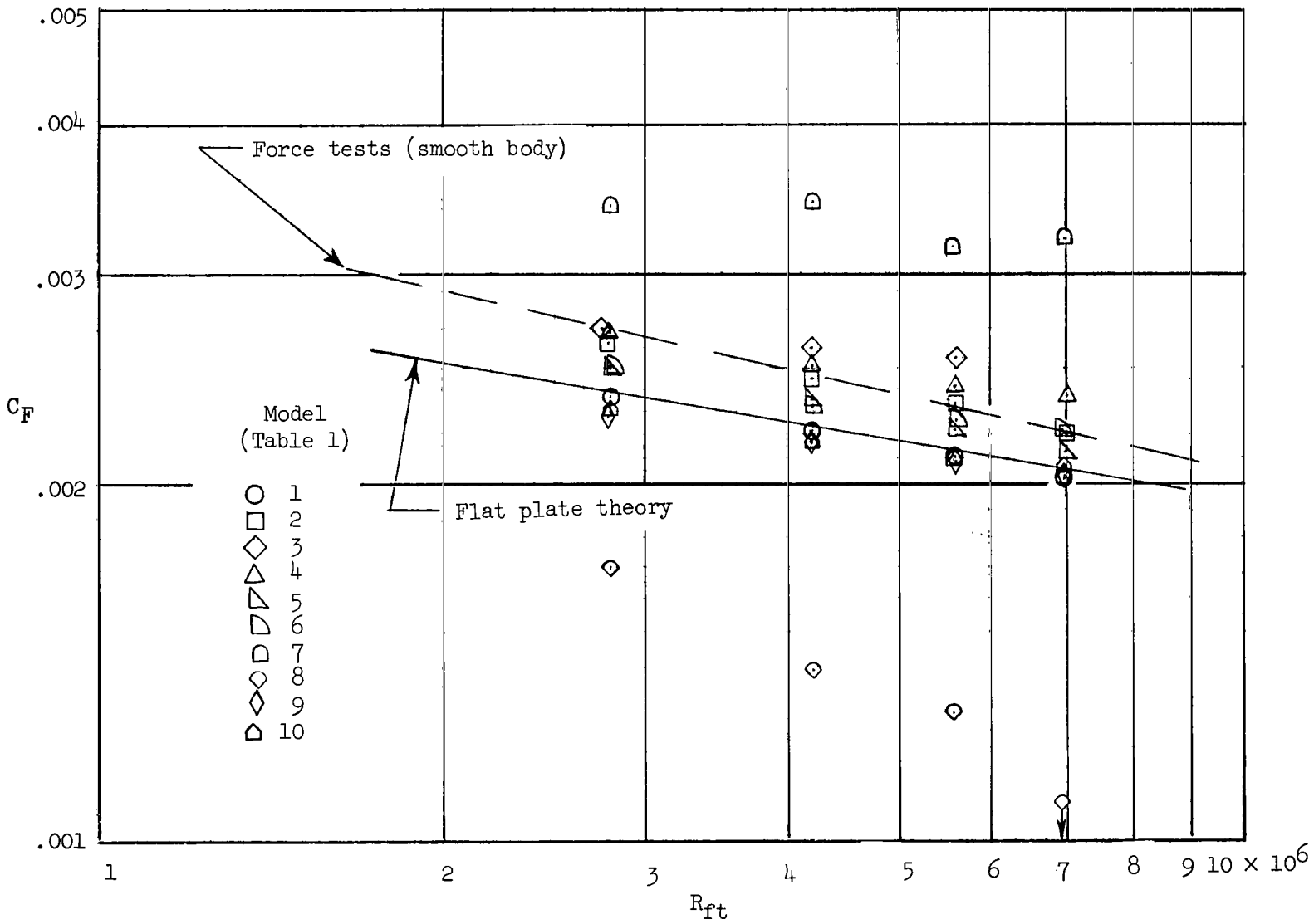

Figure 13.- Effect of surface roughness on average skin-friction coefficient. $M_\infty = 1.61$.

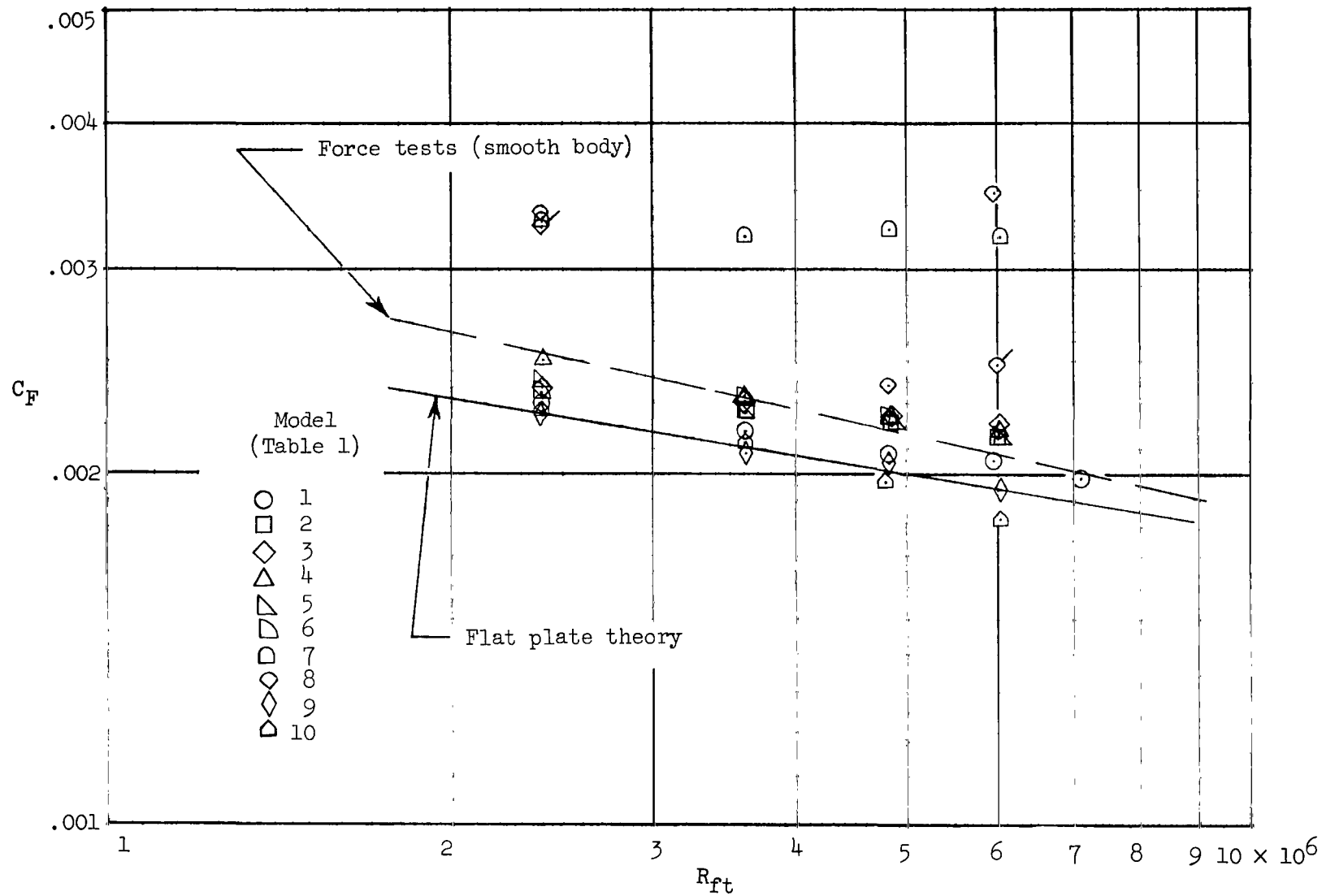

Figure 14.- Effect of surface roughness on average skin-friction coefficient. M_∞ = 2.01.
Flagged symbol indicates data taken at alternate survey station.